universität wien

MASTERARBEIT / MASTER'S THESIS

Titel der Masterarbeit / Title of the Master's Thesis

„ Studies on Micro- and Nanostructured Polyurethane Surfaces “

verfasst von / submitted by

Adriana Katharina Feldner BSc

angestrebter akademischer Grad / in partial fulfilment of the requirements for the degree of

Master of Science (MSc)

Wien, 2021 / Vienna 2021

Studienkennzahl lt. Studienblatt / degree programme code as it appears on the student record sheet:	UA 066 862
Studienrichtung lt. Studienblatt / degree programme as it appears on the student record sheet:	Masterstudium Chemie
Betreut von / Supervisor:	Univ.-Prof. Mag. Dr. Peter Lieberzeit

Contents

1. Introduction

Nanomaterials find increasing applications in many consumer products. Consequently, their release into the environment increases. Silver nanoparticles (Ag NPs) are among the most popular nanomaterials due to their outstanding properties. The effect of silver nanoparticles has been the topic of many research projects in recent years.

There are several ways of detecting nanoparticles. One possibility is the use of a sensor, such as a quartz crystal microbalance. For this application suitable receptors need to be developed. The receptor is often made of molecularly imprinted polymer (MIP) thin films. Before such a material can be used on a sensor, a series of experiments is necessary to design and optimise them. The development of the MIP material starts with the choice of a suitable polymer. Polyurethane (PU) was the material of choice for this project. PU is a versatile polymer with many applications. The material is among the most researched ones at the moment. Its application for MIPs is relatively new compared to other materials.

Throughout the process of developing a molecularly imprinted polymer thin film, several problems can occur. This includes issues concerning polymerisation, thin film preparation, imprinting and template removal. Those issues have to be resolved before the material can be used as a receptor on a mass sensitive sensor. This work focuses on problems that occurred during the MIP development in previous projects. It revolves around finding causes of those problems and tries to solve them. The focus is on the optimisation of the surface properties of the thin films and the stamps used in the imprinting process.

This Master thesis has been completed within the framework of the project “Simultaneous Multiparametric Readout for Low-Cost NP sensors” funded by the Austrian Science Fund (FWF), grant number I3568-N28, which we gratefully acknowledge.

2. Aims of the thesis

This project aimed at taking a closer look on problems that have occurred during previous projects on similar topics. It is divided into two main parts. The first one focusses on analysis of polyurethane surfaces. It deals with the frequent appearance of pores in polyurethane thin films prepared with a recipe developed by the group. The aim of the experiments is to find out if there is a connection between pore formation and certain parameters in the preparation process, such as humidity conditions, catalyst concentration or degree of cross-linking. Experiments changing one parameter in the polyurethane thin layer preparation at the time are conducted to improve the surface properties. The ideal outcome is finding a way to avoid pore formation completely and produce smooth polyurethane thin films that can be used for molecular imprinting.

The second part deals with molecular imprinting. The templates used are silver nanoparticles with diameters of 50 and 75 nm, respectively. For this task glass stamps as well as polydimethylsiloxane (PDMS) stamps were prepared according to a protocol used in the group. In order to immobilise the nanoparticles on the stamp surface it is necessary to functionalise the glass with 3-aminopropyltriethoxysilane (APTES). A problem that previously occurred in the research group is that the stamps were impossible to remove after imprinting. This was attributed to residual amine groups from the silane that react with the isocyanate groups in the polymerisation mixture. This reaction binds the stamps covalently to the polymer. The aim of this project is finding a way to block the residual amines to allow stamp removal after imprinting. Therefore, protecting groups for primary amines must be selected and tested. The sizes of the potential protection groups are of importance. They need to be small to fit in between the immobilised nanoparticles. In this work two candidates are tested. In later experiments the imprinting and template removal process is optimised. The aim is developing stamps that are easily removable and obtaining a polyurethane thin layer with nanoparticle imprints.

3. Theoretical background

3.1. Polyurethane

Polyurethanes are polymers formed by a polyaddition reaction between isocyanates and hydroxyl groups. This reaction was first discovered by Otto Bayer in 1937. [1] One of the first applications of the material was being an alternative to rubber during World War II. In the 1950s industrial production of PU began leading to exploring new applications, such as PU foams. [2] Polyurethanes are currently among the most researched materials worldwide. [3] They offer a wide range of properties. Some polyurethanes can be hard and durable, others can be soft and flexible. They find many applications in biomedicine, building and construction, textiles and several others. This is due to their outstanding properties and their versatility. [2]

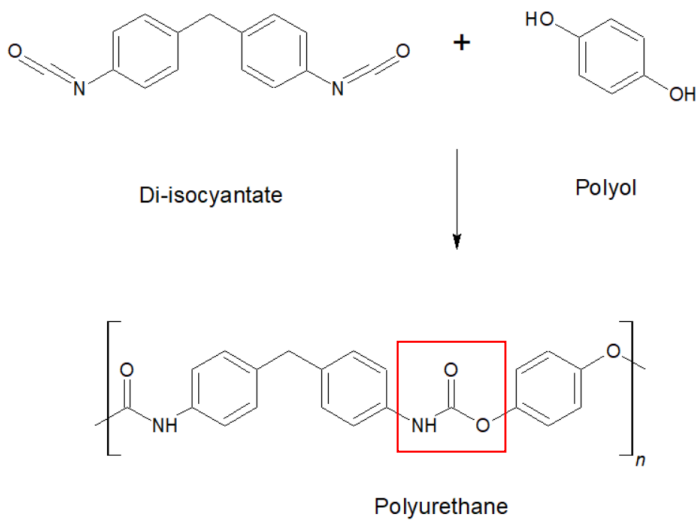

Figure 1: The polyaddition reaction with the formation of the urethane group (marked in red)

The urethane group is the characteristic repeating unit in this polymer. The reaction is depicted in Figure 1 with the urethane group marked in red. It is formed by a reaction between a polyol and an isocyanate. The hydrogen of the hydroxyl group is transferred to the nitrogen. There is no leaving group. [2]

Table 1: Overview over different PU types [2]

Polyurethanes				
Thermoplastic PU	Flexible PU	Rigid PU	PUI	Water-borne PU
Examples: Outer cases of mobile electronic devices, automotive instrument panels, power tools, medical devices, sporting goods, drive belts	Examples: Cushion materials, carpet underlays, furniture, bedding, automotive interior parts, packaging, biomedicine and nanocomposites	Examples: Thermal and sound insulators	Examples: Artificial hearts, connector tubing for heart pacemakers and haemodialysis tubes	Examples: Coatings, adhesives, sealants, binders

Table 1 shows different types of PU and their applications. Depending on synthesis, properties and application, polyurethanes can be classified into different groups. One of the major applications of polyurethanes today is the production of PU foams. Other important applications are PU coatings and elastomers. [2]

The application of polyurethanes in molecular imprinting is relatively new. In comparison with polymers made of vinylic monomers, polyurethanes are less versatile since the selection of suitable monomers is not as wide. [4]

Usually the properties of the polymer depend on the monomers used and on the degree of cross-linking. [5] Flexible and long segments lead to an elastic polymer. Polymers with a higher degree of cross-linking are more rigid. Long chains with low cross-linking produce stretchy polyurethanes. Short chains with high cross-linking are beneficial for hard polymers. [2] Additives can enhance certain properties, such as hardness, toughness and stiffness. [6] For cross-linking small polyol molecules with two or more hydroxyl groups are used. [2] Traditional polyol monomers are made from petroleum sources. Recently environmental concerns led to the research on polyols from renewable sources. Polyols from vegetable oils have been in the centre of attention for this application. [7] Apart from the polyols, isocyanates are necessary. Aromatic isocyanates are a popular choice since they are more reactive than aliphatic ones. [2]

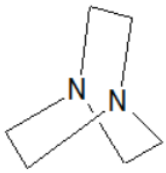

Figure 2: Chemical structure of the catalyst 1,4-diazabicyclo[2.2.2]octane (DABCO)

The reaction is very slow at room temperature. It is often accelerated by a catalyst. There are two main categories of catalysts used for PU synthesis: metal catalysts and amine compounds. Usually complexes of the metals zinc, lead, bismuth, mercury and tin are used. Examples for popular amine catalysts are 1,4-diazabicyclo[2.2.2]octane (DABCO) and triethylenediamine (TEDA). [2] DABCO was used in parts of this project and is depicted in Figure 2.

3.2. Molecular imprinting

Biomolecules such as enzymes, antibodies and hormone receptors fit perfectly to their target molecules. This makes them very good recognition systems in analytical or biomedical chemistry. They have, however, one major drawback, which is their lack of stability outside of their native environment. This makes it hard or even impossible to integrate them in industrial processes. Additionally, they are often expensive and not easily accessible. For certain molecules there might not even be a suitable receptor commercially available. [4]

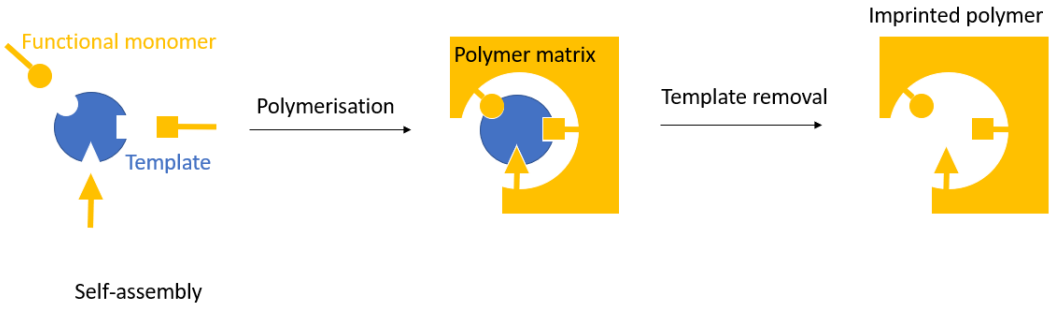

Figure 3: Schematic depiction of molecular imprinting

Molecular imprinting is a strategy to produce exact imprints of an analyte in a polymer matrix. It allows to produce artificial receptors for a wide range of target analytes based on synthetic polymers. The general procedure of molecular imprinting is depicted in Figure 3. Functional monomers are polymerised around a template. The matrix is stabilised by a cross-linker which connects the polymer chains. The template can interact with the monomers via covalent or

non-covalent interaction. After template removal stable cavities that are complementary to the template in their size, shape and functional groups remain in the polymer matrix. Selective recognition and rebinding of the target analyte occur in the imprints. [4]

Molecularly imprinted polymers mimic important characteristics of bioreceptors. The most important one is selective recognition. However, there are certain differences: In peptides the amino acids are arranged in a fixed pattern. In polymers the arrangement of the monomers is often random. Another difference is the amount and distribution of binding positions. While molecularly imprinted polymers can form a great number of binding positions, bioreceptors have fewer, often only one. An advantage of the polymers compared to biomolecules is their stability in various media. They are applicable for various target molecules. Especially the imprinting of small organic molecules is well established today. The shape of a MIP material can be adjusted to a certain application. They can be prepared in different forms, such as thin films, micro- and nanospheres and nanocomposites. [4]

MIPs are used as materials for selective molecular recognition. Their properties make them suitable materials for receptors in chemosensors. Other applications of MIPs include catalysis, chromatography or solid-phase-microextractions. MIPs are compatible with many fabrication techniques and engineering conditions, such as laser ablation and surface patterning. Another advantage of the material is the low manufacturing cost in comparison to bioreceptors. This makes MIP materials suitable for so-called plastic antibodies. [4]

Most MIPs are based on organic polymers. Popular monomers contain vinyl groups and are polymerised by radical polymerisation. This is due to the wide range of vinylic monomers with various functional groups to choose from. Monomers are chosen to obtain a polymer with suitable structure and properties. In recent years also other polymers, such as polyurethanes have been used for MIP preparation. In comparison to vinylic polymers they are limited in their versatility because there are fewer monomers available. Also, the imprinting of sol-gels, such as silica and titanium dioxide has gained in relevance. In recent years also composite materials found their application in MIP preparation. They combine the advantages of MIPs with the special properties of the composite material. [4]

Monomer selection

The functional monomers that interact with the template during polymerisation are selected according to two strategies. The first one is based on the fact that selective recognition in nature occurs via weak non-covalent bonds. It is the method used in most approaches because many monomers can form non-covalent interactions to various templates. This so-called self-assembly method has the advantage of being compatible with a wide selection of monomers that can interact with almost all templates. Possible ways of interaction are hydrogen bonds, ionic interactions, Van-der-Waals forces and hydrophobic interactions. Typically, the monomers must be used in excess. The binding of the template is governed by an equilibrium. As a result, the binding sites show heterogeneous distribution. The template is removed by solvent extraction and the analyte can selectively rebind via the same interactions. [8]

The second strategy is based on the formation of covalent bonds between monomer and template. This bond is already formed prior to the polymerisation. For template removal

cleavage of the covalent bond is necessary. Rebinding of the analyte occurs via covalent bonds as well. [9] The monomer-template complex is stochiometric. In general, this approach is more complex, since it involves additional steps: the formation and cleavage of the bond. Rebinding is often slower than in the non-covalent method because covalent bonds take longer until they are formed. [4]

There is also a hybrid strategy called semi-covalent imprinting. In this approach the templates interact with the monomers via covalent bonds, but rebinding occurs via non-covalent interactions. [10]

Imprinting strategies

There are several imprinting strategies. Which one to choose depends mainly on the template. The simplest form of MIP synthesis comprises of a template, at least one functional monomer, a cross-linker and if needed a suitable solvent. Most polymerisation reactions require a catalyst, irradiation or a heat source. [4]

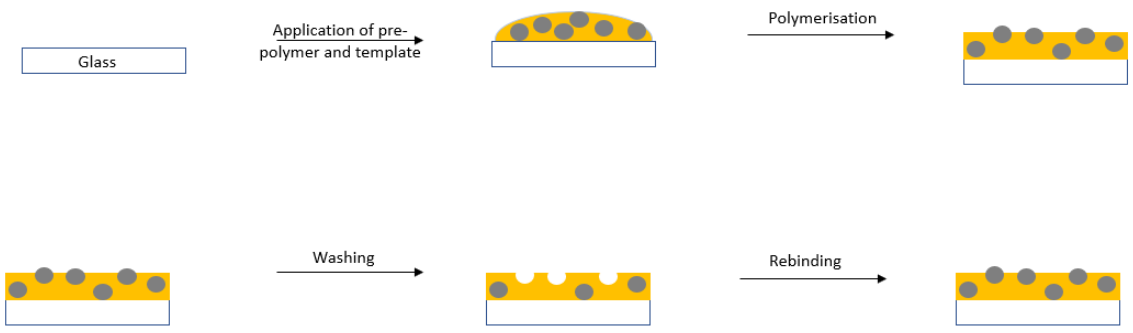

Figure 4: Schematic depiction of bulk imprinting

In bulk imprinting, which is depicted in Figure 4, the template is added directly to the polymerisation mixture. The polymer network forms and encloses the templates. After polymerisation the templates are removed by washing. This method is easy to execute and is mostly suitable for imprinting with small molecules. Drawbacks are slow binding kinetics and poor mass transfer. Since the template is added to the mixture, many binding sites are in the bulk and thus not accessible. [11] Bulk imprinting is limited to templates that are soluble in organic solvents used for the polymerisation. This makes it an unsuitable method for imprinting biological macromolecules. False signals can be caused by leakage of enclosed templates during analysis or binding of matrix components on non-specific binding sites. [12]

To extend the applications of molecularly imprinted polymers to larger templates, surface imprinting was developed. As the name suggests, the imprints are located on the polymer surface only. In contrast to bulk imprinting the templates are not added to the polymerisation

mixture. They are placed on the polymer surface and often pressed into the polymer layer with a stamp. This allows also for the diffusion of larger molecules into the polymer network. Surface imprinted polymers are very robust. In general, fewer binding sites can be formed compared to bulk imprinting because they are limited to the polymer surface. Another drawback is that there are no imprints of the whole molecule since only a part of the template is pressed into the surface. [11] Surface imprinting can be divided into different strategies.

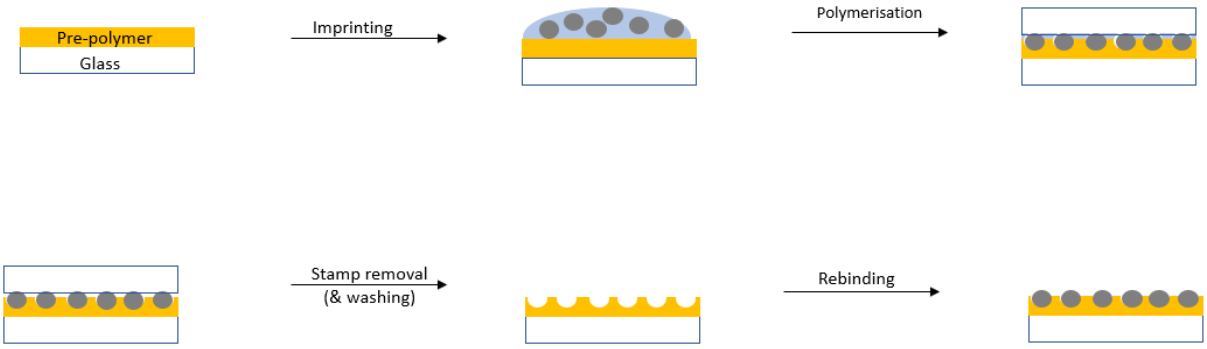

Figure 5: Schematic depiction of sedimentation imprinting

One form of surface imprinting is sedimentation imprinting. Figure 5 shows the process. Here the solution or suspension containing the template is drop coated onto the pre-polymer and covered with a stamp. The templates sediment into the polymer layer. The solvent evaporates with time. A washing step is necessary to remove the template from the hard polymer. [13]

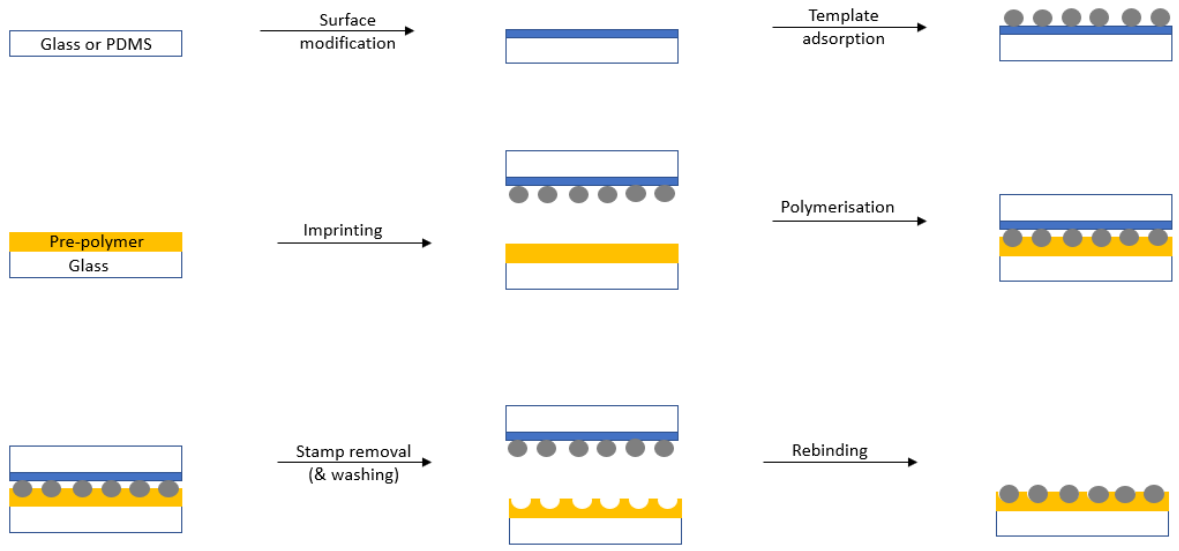

Figure 6: Schematic depiction of stamp imprinting

Stamp or microcontact imprinting is another form of surface imprinting. The process is depicted in Figure 6. The template is adsorbed on a stamp which is then brought into contact with the polymer surface. Stamps can be made from elastomeric materials, for example polydimethylsiloxane, or harder materials, such as glass. Sometimes, it is necessary to chemically modify the stamp surface to adsorb or bind the template. Then the stamps are coated with the solution containing the template molecules. They are dried to remove the solvent before use. A pre-polymer is deposited on a suitable substrate. The stamp is placed on the pre-polymer with the templates facing downwards. Then the polymer is cured. The stamp is removed from the fully cured polymer and, if necessary, remaining templates are removed by washing. Glass is an attractive material for stamp preparation: Since the material is optically transparent it is ideal for the preparation of polymers that require UV-irradiation. Also, glass surfaces can easily be modified with various organic compounds. The choice of compound used for modification depends on the template and the interactions needed for immobilisation. [14]

3.3. Nanoparticles

Particles in the size range of 1-100 nm are referred to as nanoparticles. These particles can be formed naturally or incidentally. However, they can also be produced intentionally for industrial purposes. These engineered materials are increasingly used for different commercial products, such as catalysts, cosmetics and drug carriers. Nanoparticles can appear in the unbound state or form aggregates or agglomerates. [15] Due to their dimensions, the properties of nanomaterials differ from those of the same bulk material. This can be useful for certain applications, but it may also have a negative effect on biological systems. Their small size allows for easy uptake into and interaction with biological tissue. Some nanoparticles can

move through the body, accumulate in organs and penetrate cell walls. In addition, their large surface area and ability to generate reactive oxygen species increases their toxicity. The smaller the particles get, the higher their ratio of surface area to volume. [16]

Silver nanoparticles

The antibacterial properties of silver have been known for centuries. It has been used for wound healing or purification and conservation of liquids, such as water, wine and milk. [17] Suspensions of colloidal nanosilver have been used in medical applications for almost one century. [18]

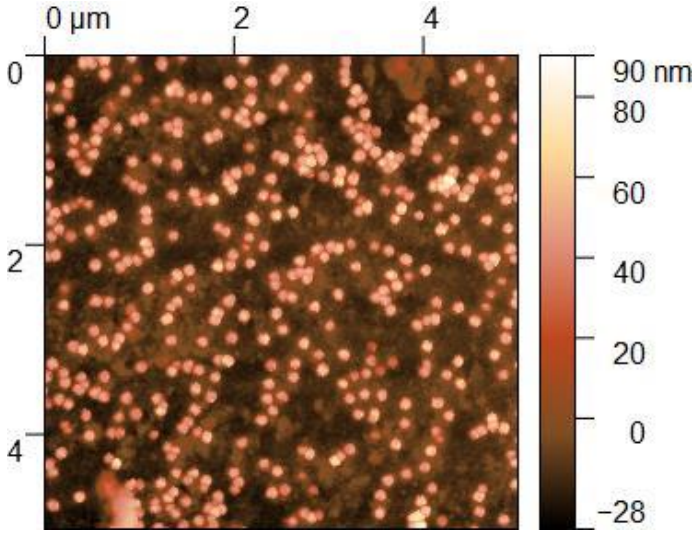

Figure 7: Silver nanoparticles (75 nm) adsorbed on glass

Today silver nanoparticles are one of the nanomaterials used most in consumer products. [19] An AFM image of silver nanoparticles adsorbed on glass is shown in Figure 7.They are known for their antimicrobial properties, making them excellent biocides. [20] In addition to that, they have high thermal and electrical conductivity making them useful for applications like microelectronics. [19] Silver nanoparticles can be found in cosmetics, deodorants, paints filters, textiles, food packaging, functionalised plastics, medical devices, wound dressings, refrigerators, washing machines and detergents. [21]

The consequence of the widespread use of Ag NPs is the increased exposure of organisms and the environment to these nanoparticles. The exposure can occur during manufacturing, use of products containing Ag NPs or when end products are disposed of. Release into the environment happens mainly via wastewater making aquatic ecosystems the most exposed ones. [22]

Ag NPs in the environment

The fate of the silver nanoparticles in the environment depends on the surroundings. Different environmental factors, such as ionic strength, the pH of the medium or the interaction with

organic matter can alter the properties of particles and their toxicity in different ways: Oxidation leads to the release of toxic Ag^+ ions. The dissolution and release of Ag^+ depends on the particle size. The smaller the particles are, the more ions they release. Additionally, the pH of the surrounding environment can influence the number of ions dissolving from the nanoparticles. [23]

High ionic strength of the surrounding medium promotes aggregation. Silver nanoparticles usually have a negative surface charge in aquatic conditions. This makes them naturally repulse each other. In the presence of positively charged ions this surface charge can be eliminated. Especially divalent cations, such as Ca^{2+} or Mg^{2+} cause aggregation of silver nanoparticles. The pH also plays a role in this process. When the pH of the medium is equal to the point of zero charge of the NPs, aggregates will be formed. The point of zero charge of silver nanoparticles is estimated to be around 2. This means that nanoparticles in acid conditions will tend to form aggregates. [23]

The interaction of natural organic matter (NOM) with such particles can cause various effects. NOM can be adsorbed on the particle surface. This can affect dissolution and aggregation. Adsorbed NOM can form a layer around the nanoparticles. The layer can stabilise the particles sterically and electrically and thus decrease aggregation. [24] Less dissolution takes place because the adsorbed NOM blocks oxidation sites. NOM can also decrease the dissolution of silver nanoparticles because under certain conditions it can reduce Ag^+ to Ag^0. [25]
In nature all effects named above are acting together. Naturally they will also interfere with each other. [26]

Ag NP in the body

Transformations can also occur in biological media. Biological fluids usually have high ionic strength which promotes the formation of aggregates, as mentioned above. [26] Dissolution of the NPs can occur as well in biological medium. Parts of the dissolved Ag^+ ions can precipitate as AgCl with chloride ions that are present. [27] The pH has an influence in biological medium as well. In areas with low pH, such as in the acidic stomach fluid Ag^+ and AgCl is formed more easily. [28]

Interaction with proteins leads to the formation of the so-called protein corona. This changes properties, such as surface charge and hydrodynamic radius and aggregation. Those changes also alter their way of interacting with cells. [26] The protein corona decreases the dissolution of Ag^+ and increases NP stability. However, the uptake into cells is facilitated. Inside the cell the protein corona may be lost. Without the protein layer the nanoparticles can dissolve and release Ag^+ ions inside the cells. [29]

Silver nanoparticles are cytotoxic. The mechanism cannot yet be fully explained. The most accepted hypothesis is the so-called Trojan-horse-mechanism [30]: nanoparticles are internalised into the cells. There high levels of toxic ions are released into the cytoplasm. The ions can there depolarise mitochondrial membrane, inactivate enzymes and damage lysosomes. A consequence of those processes is an increased level of reactive oxygen species (ROS). This causes damage in the cell membrane or the DNA. These changes may lead to cell death by apoptosis, necrosis or autophagy. [26] Although those transformation have a negative impact on the body, they are studied for possible applications in therapy such as

anticancer treatments. [26] Tumour cells are known to be more acidic than healthy tissue. This means that the release of Ag^+ is higher in these cells. This can cause the death of the tumour cells because of the ROS formed. [31]

Increasing dissolution of Ag NPs into Ag^+ will be harmful for the environment and human health. Ag^+ ions are known to be toxic. They interact with NADH dehydrogenase in the respiratory chain. This can result in the uncoupling of the respiration from the ATP synthase. They also bind to transport proteins which leads to proton leakage and the collapse of the proton motive force. [32] The dissolution and thus the toxicity are influenced by the aggregation of the nanoparticles. From larger aggregates less ions are dissolved than from smaller aggregates or individual particles. This is the case because in larger aggregates less surface area is available for dissolution. [33]

3.4. Atomic force microscopy

Atomic force microscopy (AFM) is a tool for analysis of surface topography. Areas in the micrometre and nanometre range can be scanned.

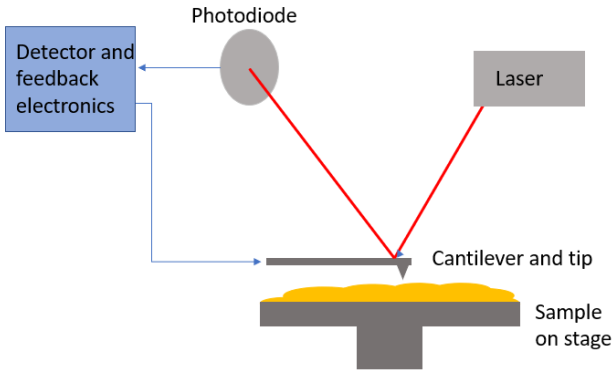

Figure 8: Schematic of an atomic force microscope

Figure 8 shows the schematic of an AFM setup. A tip mounted on a cantilever interacts with the sample surface. Height differences on the surface change the deflection of the cantilever through repulsive interactions. A laser is focused on the cantilever. From there the laser beam is reflected onto a photodiode. Changes in cantilever deflection change the position of the laser beam on the photodiode. Based on this information the software can generate a height profile image of the sample surface. The sample is placed on a stage and can be moved in x- and y-direction. A scanner is responsible for the movement of the tip across the sample. Control electronics handle the feedback between information coming out of the AFM and going back in. Vibration isolating desks are used to minimize noise caused by external vibrations. AFM setups usually also include an optical microscope to observe the sample and monitor the tip. [34]

Imaging modes

There are different modes of imaging in atomic force microscopy. This project mainly relied on contact mode and tapping mode.

Contact mode

The first imaging mode developed was contact mode. During the measurement the tip is constantly in contact with the sample. Scanning over the surface, height differences in the topography of the sample cause the cantilever to be vertically deflected. [35] Deflection is kept at a constant set point determined by the operator. Tip and sample can easily be damaged in contact mode since they are in constant physical contact. [34]

Tapping mode

Tapping mode is suitable for more fragile samples that would be damaged in contact mode. The cantilever is oscillating. The tip taps the sample as is scans across the surface. Changes in the topography of the sample surface lead to a change in the amplitude of the cantilever oscillation. These amplitude changes are monitored and minimised and ultimately used to generate the topography image. [35] The advantage of this imaging method is the gentle interaction between sample and tip. Yet, it is sensitive enough to obtain high resolution images. [34]

Peak force tapping

A relatively new imaging method is peak force tapping. Here the tip taps the surface periodically, like in tapping mode. The interaction force is measured via the cantilever deflection. The peak force is kept down by a feedback loop. With this method the operator is able to measure very small structures at high resolution. In addition to the topography, other properties, such as modulus, deformation and dissipation, can simultaneously be assessed. Soft as well as hard samples can be analysed with this method and the risk of destruction of the sample and the tip is very low. [35]

4. Materials and methods

4.1. Chemicals and equipment

For polyurethane synthesis we used the following reagents: 4,4'-diphenylmethane diisocyanate (DPDI) from Merck, bisphenol A (BPA) and phloroglucinol (PG) from Alfa Aesar. The catalyst 1,4-diazabicyclo[2.2.2]octane (DABCO) was from Alfa Aesar. Tetrahydrofuran (THF) from VWR served as the solvent for polymerisation. Other chemicals that were frequently used during the project were toluene from VWR, 3-aminopropyltriethoxysilane (APTES) from Sigma-Aldrich, dichloromethane from Roth, acetaldehyde and acetic anhydride from Merck.

Silver nanoparticle suspensions for imprinting were purchased from nanoComposix. The 50 nm particles had a diameter of 51 ± 9 nm (determined by transmission electron microscopy by the distributer) and a Ag mass concentration of 5.35 mg/mL (determined by ICP-MS by the distributer). The 75 nm particles had a diameter of 77.5 ± 9 nm and a Ag mass concentration of 5.00 mg/mL. The nanoparticles of both sizes had a polyvinylpyrrolidone surface and were suspended in Milli-Q-Water.

For PDMS stamp preparation the Sylgard Elastomer Kit was used. For glass stamps or glass substrates microscope slides from VWR were cut into pieces.

Spin coating of the polymer thin films was conducted with a spin coater G3P-8 from Specialty Coating Systems. A plasma discharger from Diener Zepto with a Balcers TPC 015 vacuum pump was used for oxidising the surface of glass or PDMS (Figure 9).

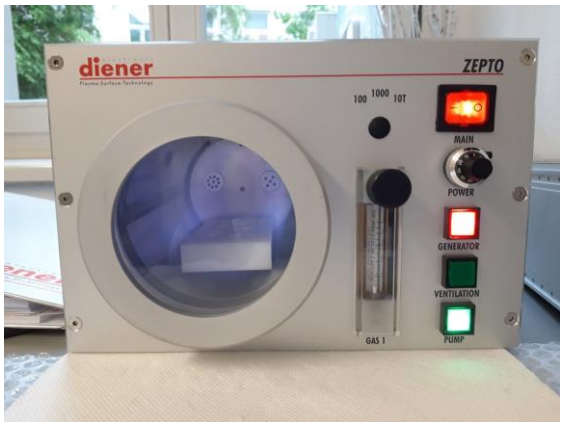

Figure 9: The plasma discharger used in the project

4.2. Sample analysis

Atomic Force Microscopy (AFM) was the main tool to analyse samples via a Bruker NanoScope VIII (Figure 10). For tapping mode measurements 0.01 - 0.025 Ohm-cm Antimony (n) doped Si tips from Bruker (model: TESPA-V2) were used. For measurements in contact mode Silicon tips on nitride levers from Bruker (model: SNL-10) were used. For peak force measurements 1 - 10 Ohm-cm Phosphorus (n) doped Si tips from Veeco (model: RTESP14) were used. Some measurements were also made on an atomic force microscope CPII from Vecco. Those measurements were all made in contact mode using Veeco NanoProbe tips (model: DNP-S1).

Figure 10: The AFM from Bruker used for sample analysis during the project

4.3. General procedures

The following procedures were frequently used for sample preparation throughout the project.

APTES functionalisation of glass plates

For certain applications the surface of glass slides had to be modified with APTES. This silane can bind to hydroxyl groups on the glass surface. Therefore, plasma treatment of the glass is required to oxidise it. The APTES modification introduces primary amine groups to the glass surface.

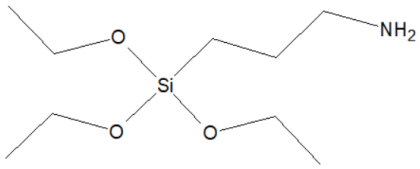

Figure 11: Chemical structure of APTES

Figure 11 shows the chemical structure of APTES. Microscope glass slides were cut into pieces of about 1x1 cm. They were cleaned with acetone in the sonication bath for 5 min. After drying the glass plates were treated in the plasma cleaner for 5 min. Afterwards, they were stirred in a petri dish filled with 1 mL APTES in 20 mL toluene for 1h. The functionalised glass plates were rinsed with toluene, ethanol and distilled water in this order.

The glass slides were used as a substrate for non-catalysed polyurethane and for preparing the glass stamps for nanoparticle imprinting.

Polyurethane synthesis

The following recipes were used for synthesising polyurethane in this project. These are the original recipes taken from other works. During the project they were adapted and optimised as described in the experimental section. Figure 12 depicts the chemical structures of the monomers and the cross-linker

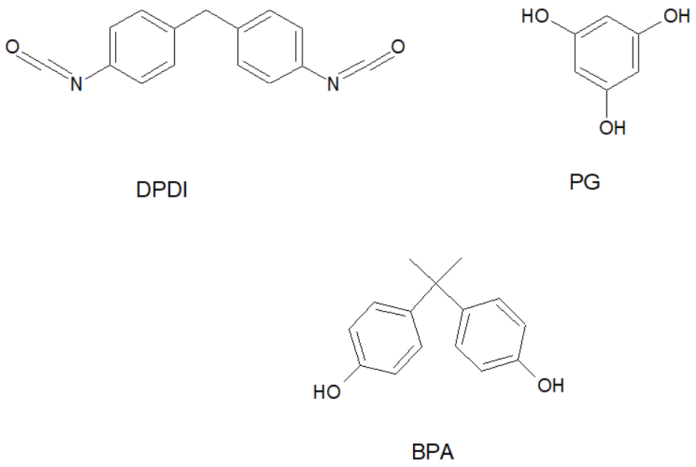

Figure 12: The monomers DPDI and BPA and the cross-linker PG for polyurethane synthesis

Non-catalysed polymerisation

For the non-catalysed polymer, a recipe from Patrick Wagner and colleagues [36] was used. This recipe was already in use in the group and known to form smooth surfaces with low tendency towards pore formation.

122 mg DPDI, 222 mg BPA and 25 mg PG were dissolved in 500 µL THF using a sonication bath. The mixture was placed in a water bath at 70°C for 200 min. Afterwards it was diluted 1:5 with THF. The diluted pre-polymer mixture was spin coated on APTES modified glass at 2000 rpm for 60 seconds. The polymer was then covered with a PDMS or glass stamp and the sample was placed between two microscope slides which were secured with clamps to apply pressure. Then it was placed in the drying cabinet at 80°C for several hours.

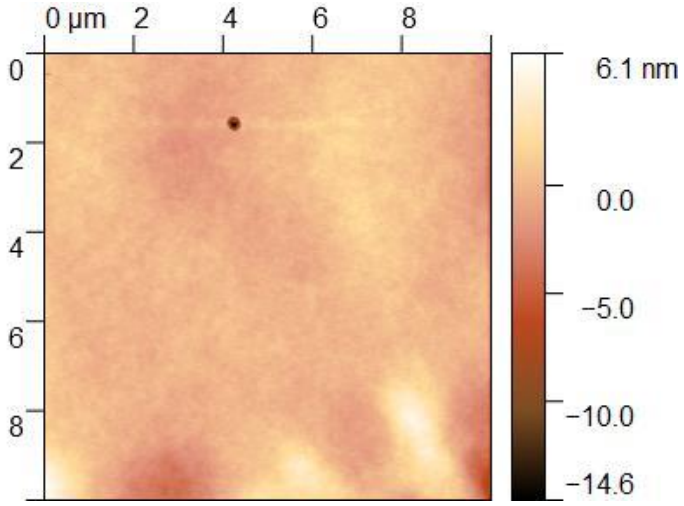

Figure 13: AFM image of the surface of non-catalysed PU

Figure 13 shows an AFM image of the polymer surface. The surface was smooth and showed hardly any pores.

Catalysed polyaddition

A polymer recipe established in two dissertations of the group [37] [38] was used for catalysed polymerisation. In the original works several different monomer ratios were tested. The recipe called “PU8” was described as the one giving the most satisfying results. Therefore, it was chosen as the basis of the experiments with catalysed polymerisation. The polymer is sometimes referred to as PU8 in this work.

200 mg DPDI, 118 mg BPA and 22 mg PG were dissolved in 200 µL THF using a sonication bath. 100 µL of the mixture were diluted 1:10 with THF. To 980 µL of 1:10 dilution 20 µL DABCO solution were added and mixed well. The polymerisation mixture was placed in a water bath at 70°C. It was frequently checked for signs of beginning polymerisation. When oligomer

formation was visible through slightly increasing viscosity, the mixture was removed from the water bath and diluted 1:10. 10 µL of the dilution were spin coated on glass plates at 2000 rpm for 10 seconds. The glass plates were previously cleaned in acetone in the sonication bath and treated in the plasma cleaner for 5 min. The polymer was then covered with a PDMS or glass stamp and the sample was placed between two microscope slides which were secured with clamps to apply pressure. Then it was placed in the drying cabinet at 80°C for several hours.

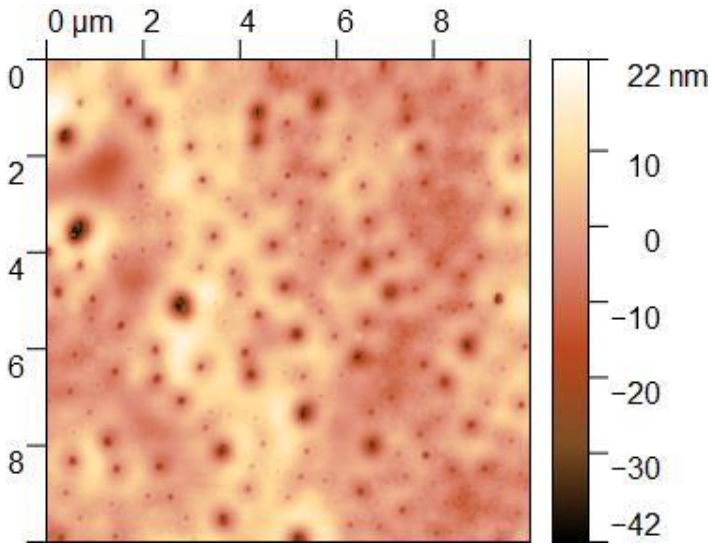

Figure 14: AFM image of PU8 prepared with 20 mg/mL DABCO solution

In the original recipe a solution of 20 mg/mL DABCO in THF was used. An AFM image of the sample surface is shown in Figure 14. Circular pores are on the surface. This problem has already been noted in the dissertations mentioned earlier. The following experiments aimed at solving this issue.

5. Experimental part

5.1. Part 1: Studies on the polymer surface

This part of the project focused on the surface topography of polyurethane samples. Especially the problem of the porous surface of the catalysed PU was addressed. The original application for the PU thin films was molecular imprinting with nanoparticles. For this application a smooth surface is necessary. The aim of this part was to find a connection between certain parameters in the process and pore formation.

Humidity experiments

One of the first hypotheses was that the pores are caused by high humidity conditions during thin film preparation and curing. High humidity conditions can be used intentionally for the synthesis of porous polymer layers. [39] The aim of the following experiments was to clarify if there is a correlation between the humidity during the curing process and pore formation in the polyurethanes used in this project.

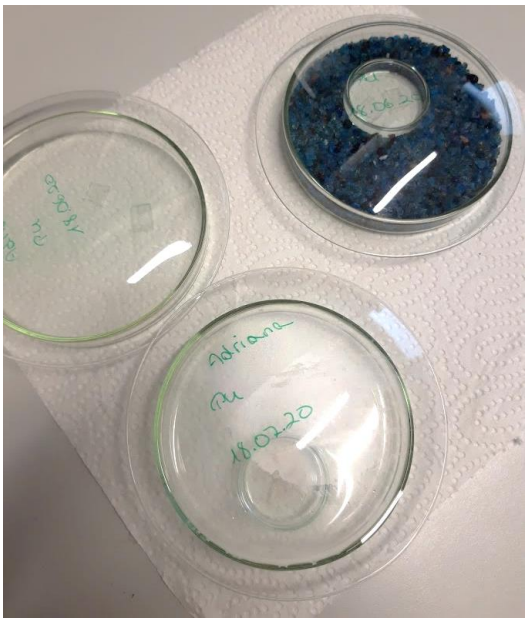

Figure 15: Set-up for the humidity experiments

For those experiments both catalysed and non-catalysed polyurethane was used. They were prepared under the same conditions and compared to each other. Figure 15 shows the set-up for the experiments. The respective polymer was prepared and spin coated as described above. The samples were then placed in small glass petri dishes inside larger petri dishes. For dry conditions the large petri dish was filled with silica gel. For humid conditions the larger

petri dish was filled with 20 mL of distilled water. The samples for “normal” - i.e. ambient - conditions were placed in a petri dish without anything else. All petri dishes were covered with a watch glass and placed in the drying cabinet overnight. The silica gel adsorbed water in the atmosphere around the dry samples. At 80°C in the drying cabinet the water in the petri dish evaporated and created a humid atmosphere under the watch glass. The samples cured under normal conditions served as controls.

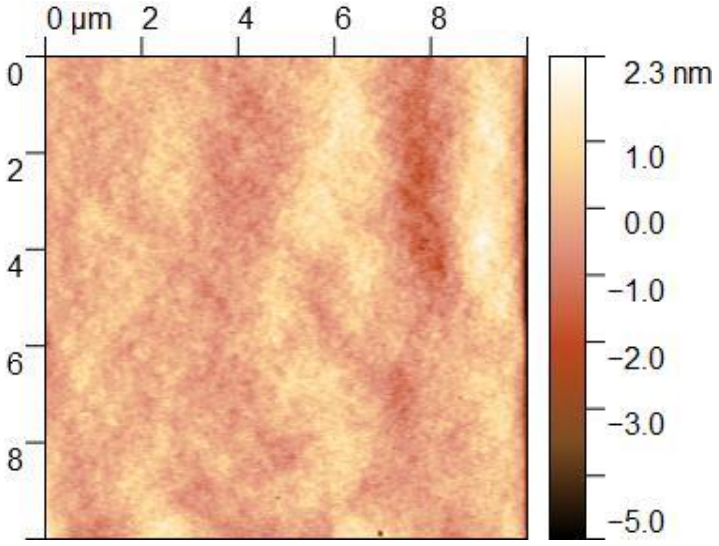

Figure 16: Non-catalysed PU in dry conditions

Figure 16 shows one result of the experiments with the non-catalysed polyurethane at low humidity. The polymer cured in dry conditions showed almost no pores, as it was expected.

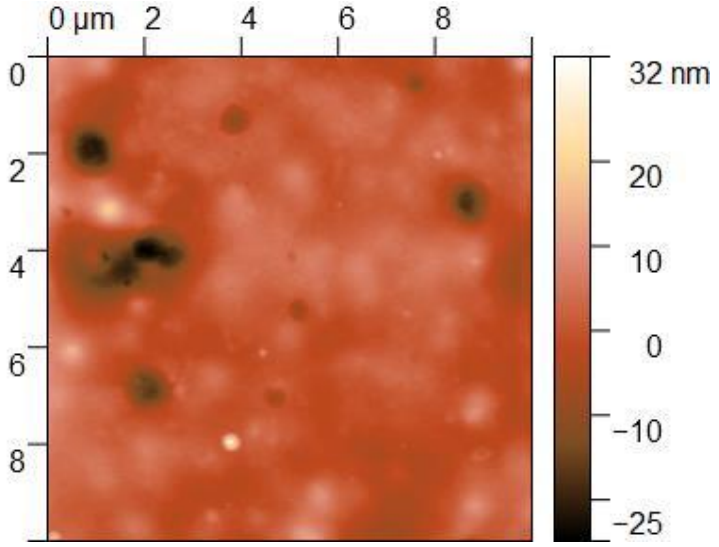

Figure 17: Non-catalysed PU in humid conditions

An example of the results for the experiments at high humidity conditions is depicted in Figure 17. At high humidity conditions during curing the non-catalysed polyurethane tended to form more pores than it did under normal or dry conditions.

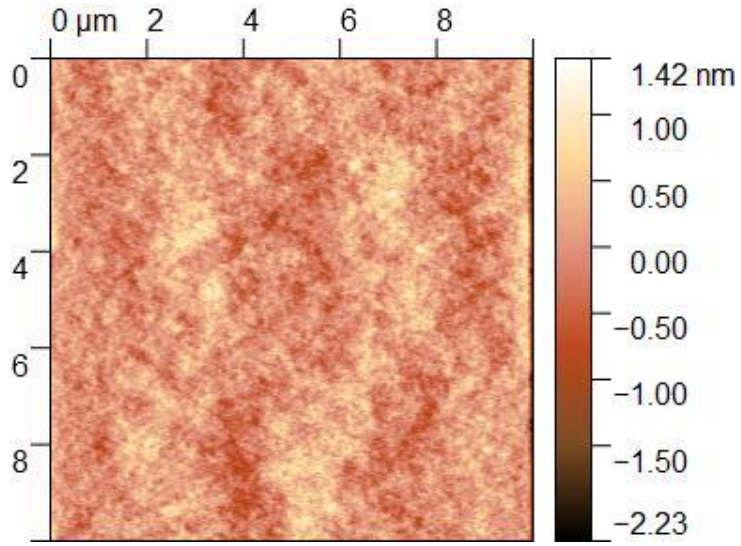

Figure 18: PU in normal conditions

The control samples prepared looked as expected. They usually exhibited a smooth surface like the one in Figure 18. Sometimes individual pores formed under ambient conditions. Especially at ambient conditions it was hard to control them in a strictly reproducible way: The conditions in the drying cabinet cannot be monitored and fluctuate with its contents and other processes, such as frequent opening of the door.

The experiment was repeated several times. All of them showed similar results to those described above. We could observe some correlation between humidity and pore formation. However, none of the samples showed similar pore density on the surface as the samples with catalysed polyurethane.

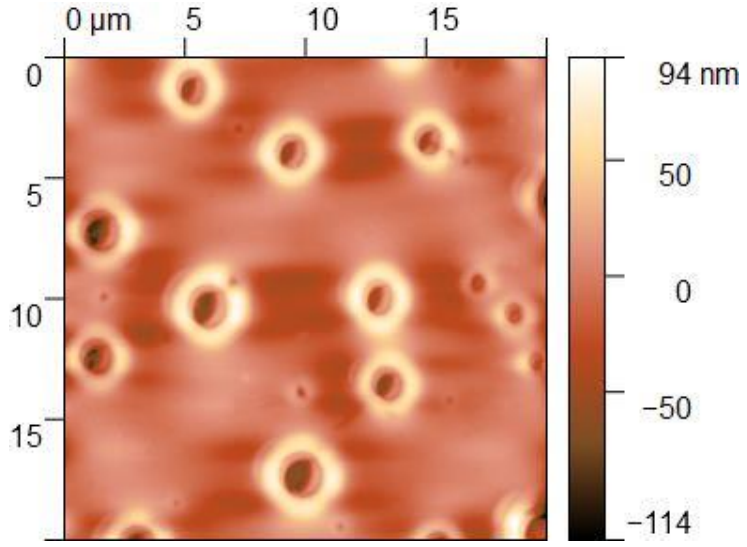

Figure 19: PU8 in dry conditions

Figure 19 shows an example of the results obtained with the catalysed polymer in dry conditions. Most of the samples had circular structures of several micrometres in diameter on the surface. The circles had a height difference of up to 200 nm to the rest of the surface and seemed to surround craters that were deeper than the surface around them. The expected effect of a reduction in pore formation was not observed.

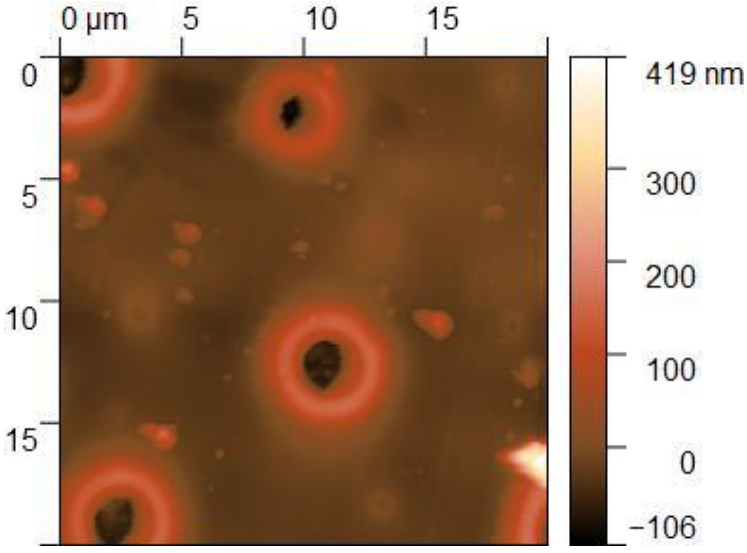

Figure 20: PU8 in humid conditions

In Figure 20 a PU8 sample prepared in high humidity conditions is shown. On the sample surface similar circular structures as on the low humidity sample were observed.

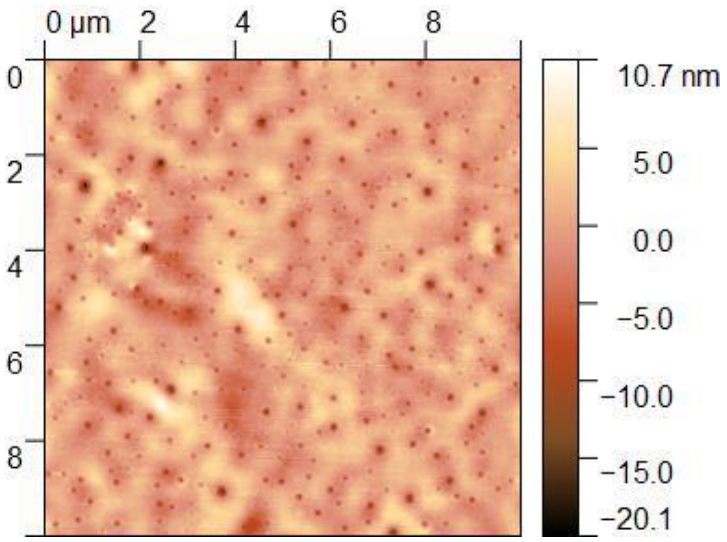

Figure 21: PU8 in ambient conditions

Figure 21 shows the AFM image of a control sample cured under normal conditions. The control sample usually showed, as expected, a very porous surface. It was always prepared at the same time and from the same polymerisation mixture, as the samples cured in humid and dry conditions. However, the ring-shaped structures around the pores were never observed on any control samples. This means that they are probably formed during the curing process and are possibly tied to the conditions during curing. However, it is not clear what effects could be responsible for those surface structures. The expected correlation between humidity and pore formation could not be observed.

Some connection between humidity and pore formation was only observed for non-catalysed PU. In comparison, catalysed PU had a more porous surface at all conditions. Given that the same monomers and solvents and the same equipment was used for preparing both catalysed and non-catalysed polymers, one can rule out contamination of the chemicals or other effects stemming from the monomers. This suggests that the problem of extreme pore formation is tied to the recipe or synthesis process of the catalysed polymer.

Optimisation of catalysed polymerisation

Therefore, we decided to optimise different parameters in the synthesis of catalysed polyurethane in order to find the factor responsible for pore formation. All spin coated samples were usually covered with a stamp. Both PDMS and glass stamps were used for all experiments. Since the choice of stamp material did not make any visible difference to the results, only one of the samples is depicted. For all experiments multiple samples as well as control samples were prepared and analysed.

Degassing

Air bubbles in the reaction mixture are an obvious source of pores. To avoid gas being trapped in the pre-polymer, the Eppendorf tube with the diluted pre-polymer was degassed immediately before spin coating. For degassing the tube was placed in the sonication bath for

10 min. The tube was handled carefully after degassing and not mixed or shaken afterwards to avoid formation of new bubbles. The recipe and procedure were otherwise not changed. The original catalyst concentration of 20 mg/mL DABCO in THF was used.

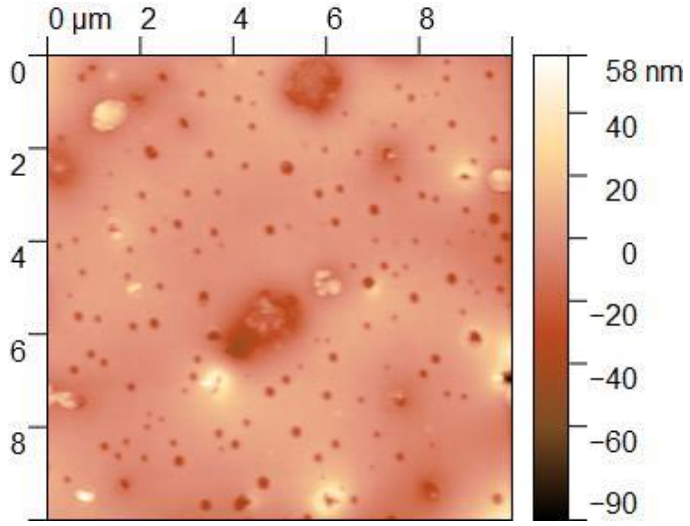

Figure 22: PU8 degassed before spin coating

Figure 22 shows an AFM image of a PU8 sample that was degassed before spin coating. The sample looks similar to the samples of the same composition prepared without degassing. This suggests that the pores are not caused by gas bubbles in the pre-polymer solution.

Reducing surface tension

Reducing the surface tension was another approach to avoid pore formation. This was expected to lead to a smoother surface of the spin coated polymer. Adding a surfactant to the polymer solution served this purpose. After dissolving the monomers in 200 µL THF, 4 mg of Triton X were added. This equals approximately 1 wt.% of the monomers. Then the polymer was prepared according to the recipe and spin coated and cured as usual.

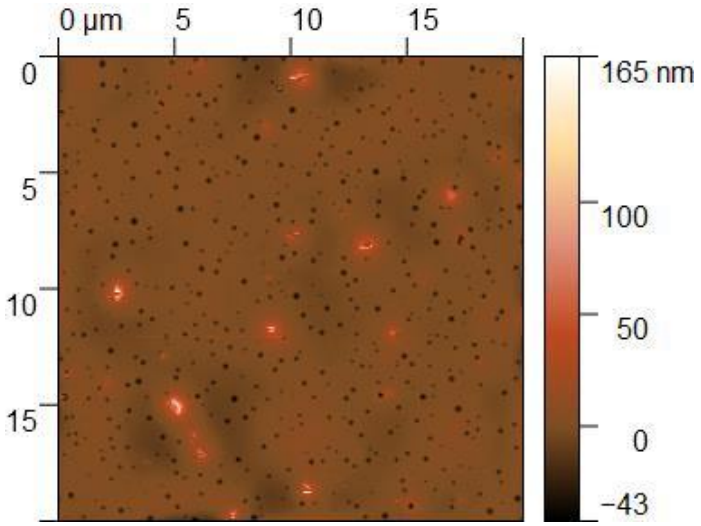

Figure 23: PU8 with 1 wt.% Triton X

Figure 23 shows the AFM image of a sample prepared with Triton X. It is evident that the surfactant did not prevent formation of the pores.

Catalyst concentration

The main difference between catalysed and non-catalysed polyaddition is, as the name suggests, the catalyst. The use of DABCO reduces the reaction time from several hours to minutes, which makes it very convenient. However, thin films prepared with catalyst seem to form more porous surfaces. Samples were prepared with catalyst solutions in a concentration range from 0.05 to 25 mg/mL in THF. In the more concentrated range of the catalyst solutions, meaning 5 mg/mL and above, the interval between the different solutions was 5 mg/mL (5, 10, 15, 20 and 25 mg/mL). Those solutions were prepared by dissolving the respective amount DABCO in 1 mL THF. For the lower concentrations, 0.05, 0.1, 0.5 and 1 mg/mL smaller intervals were chosen. Since the amount of DABCO per mL THF was very small, the solutions were prepared by diluting concentrated ones. 1 and 0.5 mg/mL solutions were obtained by diluting a 5 mg/mL solution 1:5 and 1:10 respectively. The 0.1 mg/mL solution was obtained by diluting the 1 mg/mL solution 1:10. The 0.05 mg/mL solution was obtained by diluting the 0.5 mg/mL solution 1:10. The volume of catalyst solution added was not changed. The rest of the recipe remained unchanged.

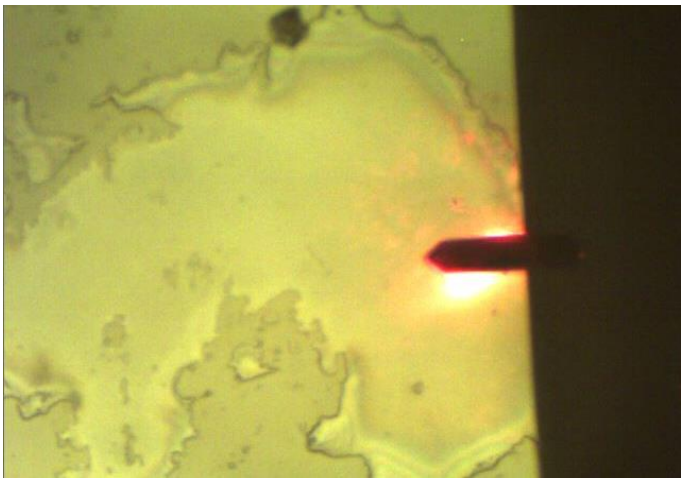

Figure 24: PU8 with 25 mg/mL DABCO; light microscope image showing also the AFM cantilever

Figure 24 shows the light microscope image with the AFM cantilever on the PU surface. This sample was prepared with 25 mg/mL DABCO solution. It is visible that the polymer did not form a layer over the whole glass surface. This can probably be attributed to the high amount of catalyst used. The polyaddition reaction is probably progressing so fast that the polymer hardens very quickly during spin coating and cannot spread during the process. This also means that that 20 mg/mL, which is used in the original recipe, is probably already the upper limit of what is reasonable for thin film preparation.

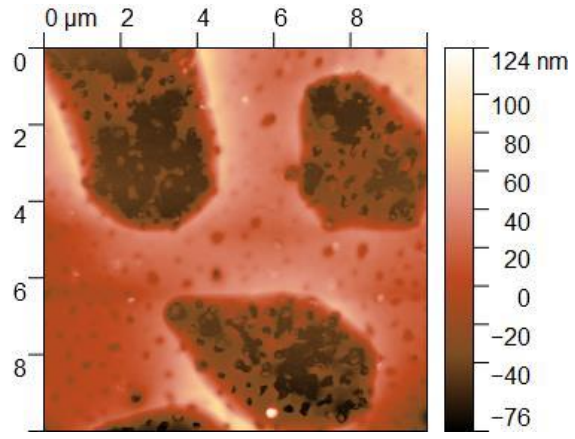

Figure 25: PU8 25 mg/mL DABCO

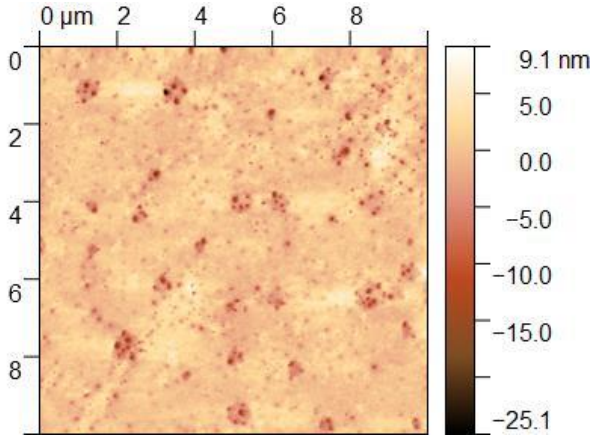

Figure 26: PU8 15 mg/mL DABCO

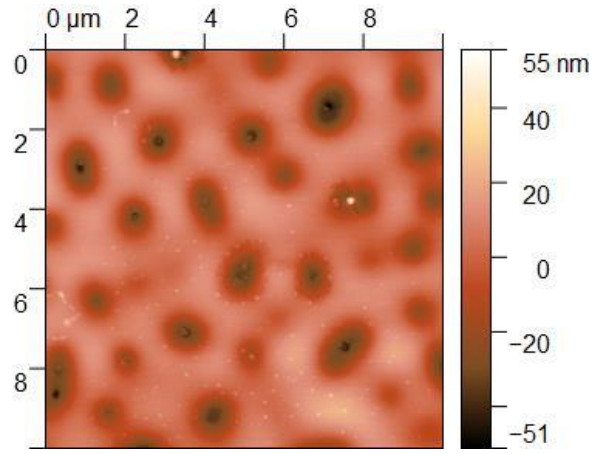

Figure 27: PU8 10 mg/mL DABCO

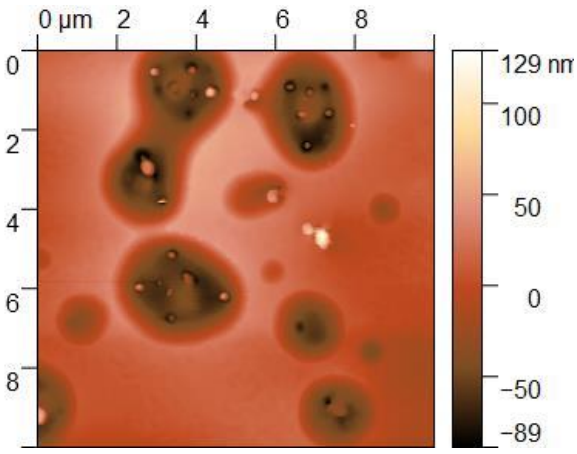

Figure 28: PU 5 mg/mL DABCO

Figure 25-Figure 28 are AFM images of the sample surfaces in the DABCO concentration range 5-25 mg/mL. An image of a control sample prepared with a 20 mg/mL catalyst solution is not included, because those samples looked similar to the example presented before. The AFM images clearly demonstrate that pores in the micrometre range formed over the whole surface. The pores looked different for all samples. In this concentration range no clear correlation between the pore formation and the DABCO concentration was visible. Those AFM images only suggest that the pores are less densely distributed on the sample surface for low concentrations as is visible in Figure 28 where a 5 mg/mL solution was used.

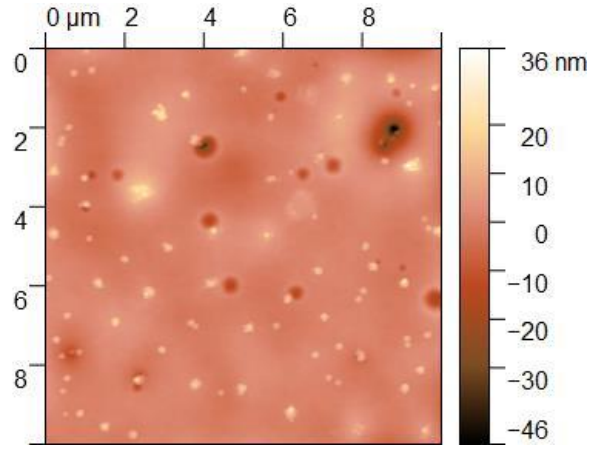

Figure 29: PU8 1 mg/mL DABCO

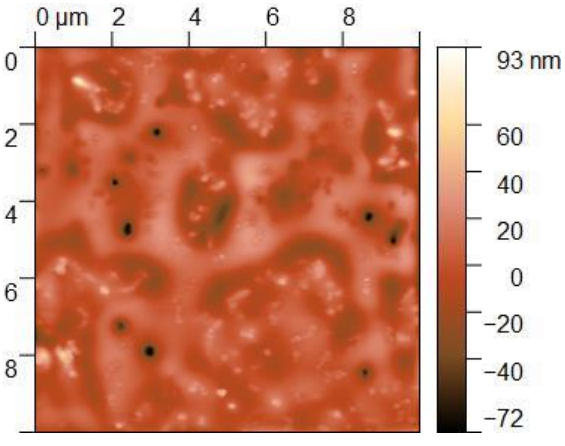

Figure 30: PU8 0.5 mg/mL DABCO

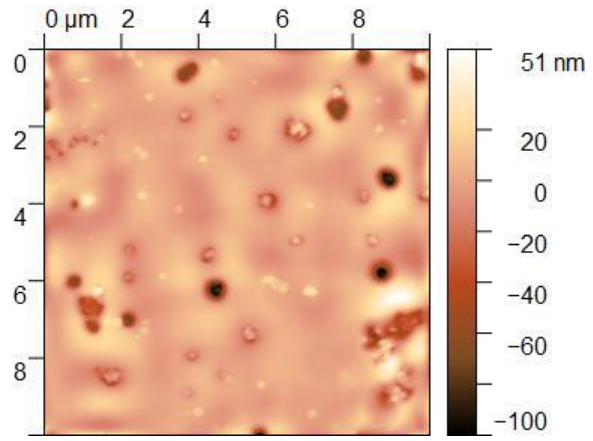

Figure 31: PU8 0.1 mg/mL DABCO

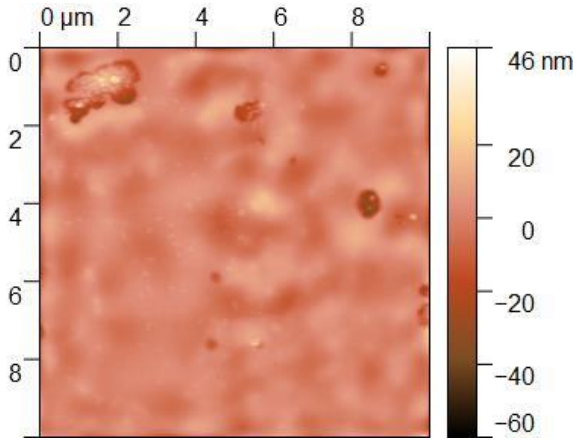

Figure 32: PU8 0.05 mg/mL DABCO

Figure 29 - Figure 32 show the results of the samples prepared with lower concentrations of the catalyst. It seems that at low concentration fewer pores are formed, but pore formation could not be prevented completely. The pores are not distributed as densely on the surface as they are at higher concentrations. However, layer homogeneity and smoothness were decreased which can especially be seen in Figure 30. Additionally, when only small amounts of catalyst are used, the reaction time increases. The advantage of the catalysed reaction which is the short pre-polymerisation time is lost.

Pore formation in catalysed polyurethane is still unpredictable and random. The results above suggest that there is a connection between the catalyst concentration and the pore formation in polyurethane. However, this is at the present moment only an assumption. Those results do not give enough evidence to make a definitive statement. More experiments need to be carried out in this area to prove this theory.

Bulk polymer

Another possibility is that the pores were formed during spin coating. The solvent is rapidly evaporating in the process which could cause the voids. To check if the pores originated from spin coating, different polyurethane bulk samples were prepared. The polymers were prepared according to the original recipe and left on the water bath until they reached a gel-like state and did not move when the tubes were inverted. The open Eppendorf tubes were placed in the drying cabinet at 80°C until the solvent had evaporated. Catalyst solutions with concentrations of 5, 10, 15, 20 and 25 mg/mL were used. The dry samples were cut into small pieces with a knife and analysed in the light microscope.

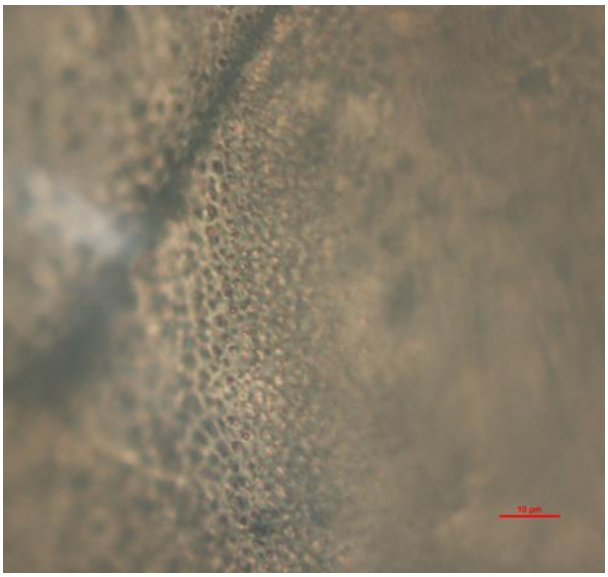

Figure 33: Bulk PU8 20 mg/mL DABCO (100x magnified)

The image of the sample prepared with 20 mg/mL can be seen in Figure 33. All bulk polymers had a similar porous structure which means that the pores form during the polymerisation independently of the spin coating process.

Concentrated polymer

Another concern was the relatively high amount of solvent in the polymerisation mixture. It was shown above that solvent evaporation during spin coating was not responsible for the porous structure. However, the samples still contained a high amount of the volatile solvent. Fast evaporation of the solvent from the pre-polymer solution could cause the formation of voids in the spin coated polymer as well as in the bulk polymer samples. To examine this possibility, samples were prepared using the concentrated stock solution. For those samples the usual amounts of the monomers were dissolved in 200 µL THF. 10 µL of a 20 mg/mL DABCO solution in THF was added and the tube was placed on the water bath at 70°C. The mixture was not diluted any further. One sample was taken from the water bath after a few minutes and drop coated on glass slides and cured at 80°C. The second sample was left on the water bath until it was fully polymerised.

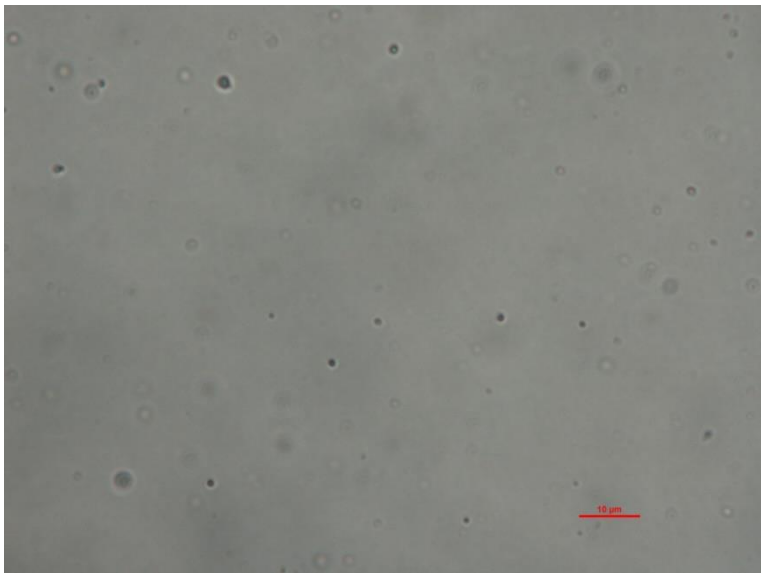

Figure 34: Concentrated PU8 drop coated (100x magnification)

All samples were observed in the light microscope. The picture of one of the drop-coated samples is presented in Figure 34. All samples prepared by drop coating revealed pores in the micrometre range.

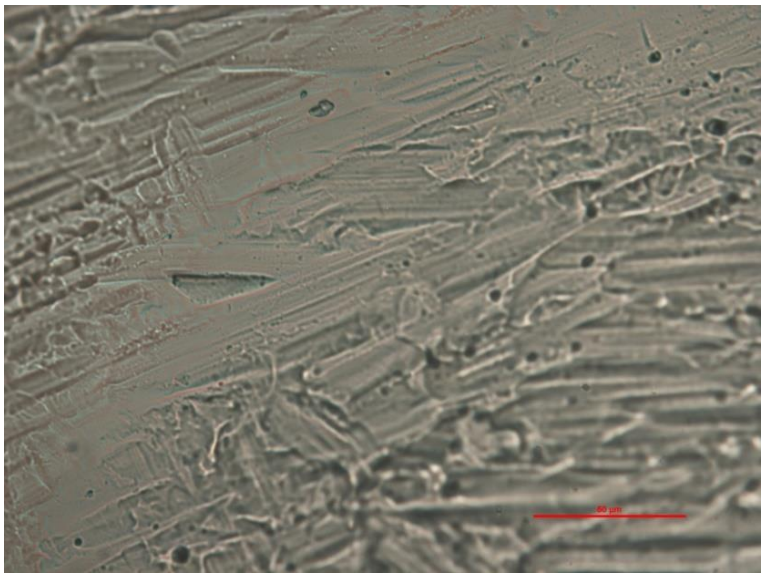

Figure 35: Concentrated bulk polymer (50x magnification)

Figure 35 shows the light microscope image of the bulk polymer. This sample as well had a porous structure. Since all the samples prepared with a minimum amount of the solvent had pores, it can be assumed pore formation is independent of the amount of solvent in the polymerisation mixture.

Modified recipe

The original recipe dissolves the monomers in a relatively small amount of solvent. It takes approximately 15 min in the sonication bath to fully dissolve them before adding the catalyst. In those 15 min polyaddition reactions can already start, which makes the process inhomogeneous. Another factor that could contribute to inhomogeneities is the fact that the mixture was not stirred during pre-polymerisation. Given that the catalysed reaction happens rather quickly this could also lead to inhomogeneous polymerisation in the solution. The numerous diluting steps throughout the synthesis process are another potential source of inhomogeneity.

To rule out the problem of possible inhomogeneous polymerisation a modified recipe was established. The isocyanate and the polyols were dissolved separately to avoid polyaddition before the monomers were fully dissolved. Smaller amounts of the monomers were dissolved and a larger amount of solvent was used which made the 1:10 dilution step in die original recipe obsolete. This also facilitated dissolving. The catalyst was added to the polyol monomer solution which means that the catalyst was introduced to the reaction at the same time as the monomers were combined and polyaddition started. Stirring during pre-polymerisation ensured homogenous mixing during the reaction. The end concentration of all components was maintained.

42 mg DPDI were dissolved in 500 µL THF. In a second tube 25 mg BPA and 5 mg PG were dissolved in 500 µL THF. 20 µL of the DABCO solution were added to the solution containing the phenol monomers. Then the two solutions were combined and mixed. A magnetic stirring bar was added and the tube was placed in the water bath at 70°C. When signs of polymerisation were visible (i.e. onset of gelation), the pre-polymer solution was taken out of the water bath. 100 µL were diluted 1:10 and spin coated on clean glass slides. The samples were covered with PDMS stamps or glass stamps and placed between two microscope slides secured with clamps. Then they were placed in the drying cabinet at 80°C overnight.

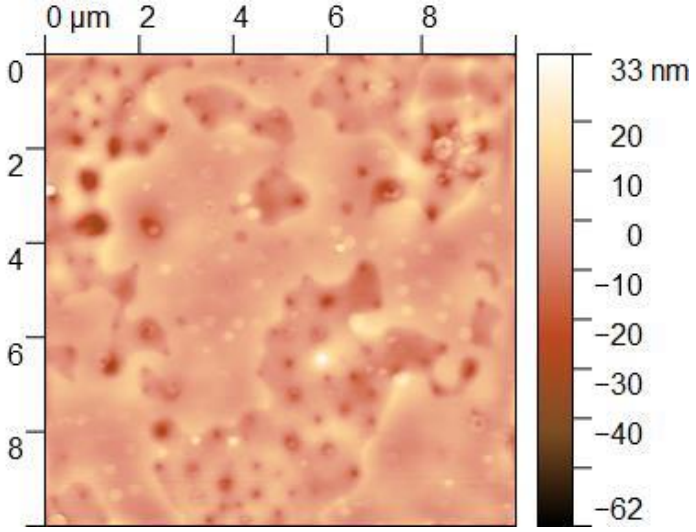

Figure 36: PU8 prepared with the modified recipe and a 20 mg/mL DABCO solution

As can be seen in Figure 36 the polymer layer still has a very porous surface. This means that inhomogeneities occurring during polymer synthesis are not responsible for the porous structures of the thin films.

Cross-linker

The effect of the amount of cross-linker in the polymer was examined. The ratio between the polyol monomers BPA and PG, which is the cross-linker, was varied. The total amount of hydroxyl groups in the reaction mixture was kept constant. Since bisphenol A contributes two hydroxyl groups and phloroglucinol three the amounts of the monomers had to be adjusted accordingly. For those experiments the modified recipe and a DABCO concentration of 20 mg/mL were used. The amount of DPDI was constant at 42 mg. The used amounts of BPA and PG are listed in Table 2. The original amounts were 5 mg PG and 25 mg BPA and were used for the control sample.

Table 2: Amounts of bisphenol A and phloroglucinol

PG [mg]	BPA [mg]
7	19
5	25
3	31
1	37
0	40

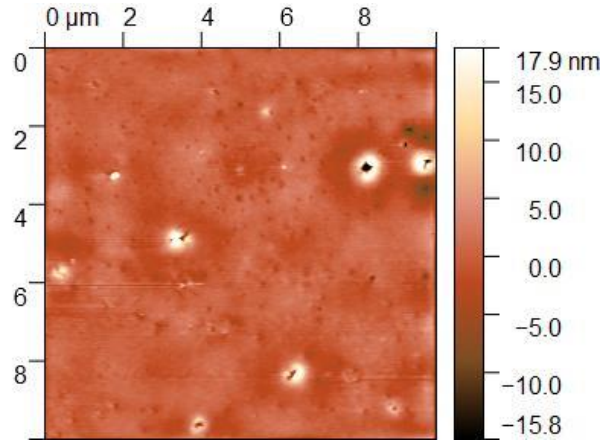

Figure 37: PU8 with 0 mg PG

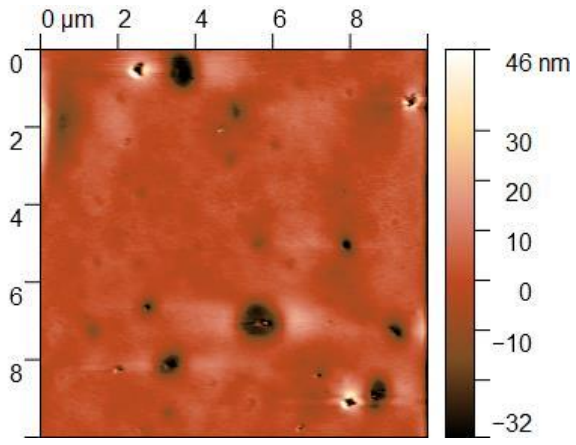

Figure 38: PU8 with 1 mg PG

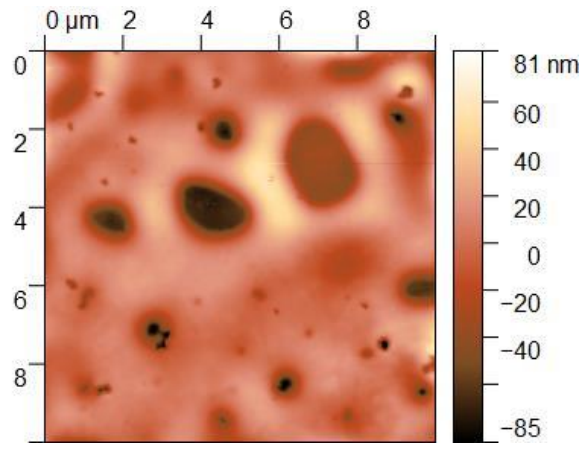

Figure 39: PU8 with 3 mg PG

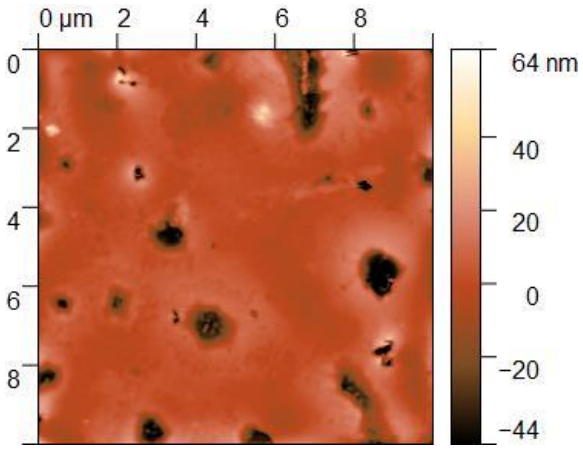

Figure 40: PU8 with 7 mg PG

Figure 37-40 summarise the AFM images of the samples (except the control sample). All polymers containing PG exhibit large pores that do not seem to correlate with the degree of cross-linking. The pores in the sample prepared without PG are smaller. Changing the amount of the cross-linker did not lead to polymers without pores.

Water content of solvent

The effect of different water contents in the solvent used for polymer synthesis was examined. The modified recipe was prepared with THF with different water contents. Dry THF was prepared by storing the solvent over a molecular sieve and under argon atmosphere. The control sample was prepared as usual with the THF taken directly from the storage bottle it was purchased in. 50 µL water were added to 5 mL THF to monitor the effect of a wet solvent.

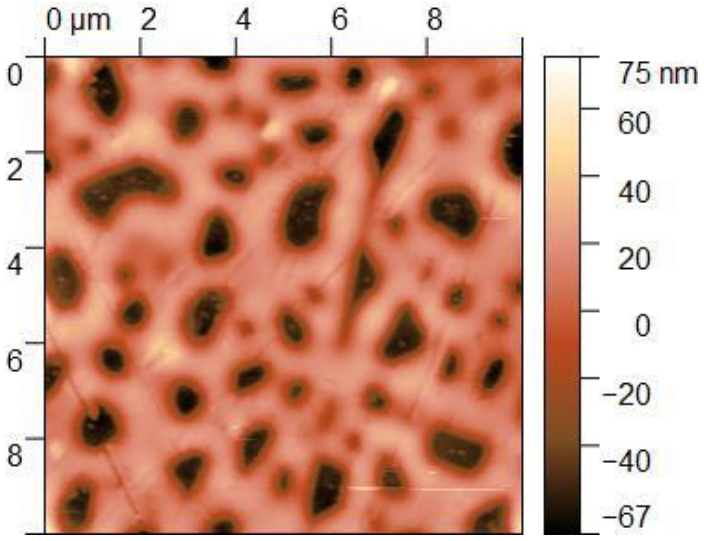

Figure 41: Modified PU8 recipe with dry THF

The sample prepared with the dried solvent (Figure 41) revealed large non-circular holes throughout the whole surface. The expectation that a dry solvent would decrease the pore formation was not met.

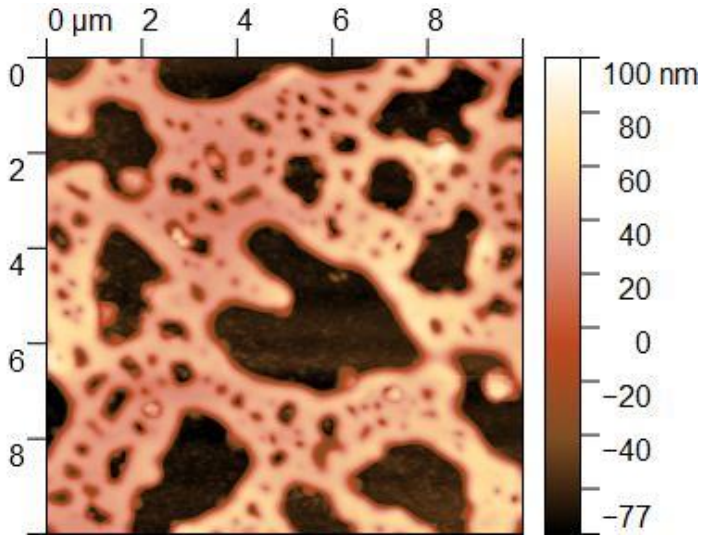

Figure 42: Modified PU8 recipe with wet THF glass

The effect of a higher water content in the solvent is evident in Figure 42. Here the polymer formed many large holes in addition to the usual pores. This is another evidence that water in any step of the process causes inhomogeneities and pores. However, water alone cannot be responsible for the pores since the samples prepared with the dry solvent were porous as well.

5.2. Part 2: Molecular imprinting and stamp optimisation

The second part of the project focused on preparing stamps for molecularly imprinting PU with silver nanoparticles. Glass stamps and PDMS stamps were used and optimised. During previous projects of the group, the stamps were sticking to the polymer and thus could not be removed after imprinting. This effect was attributed to APTES used in stamp preparation. APTES is necessary for immobilising the NPs on glass or PDMS. The terminal amines of APTES are believed to react with the isocyanate groups of the PU monomers. This would bind the stamps covalently to the polymer. The aim was to find a protecting group for the amine groups to prevent this from happening. Since it was not possible to obtain thin films without pores with catalysed polyaddition, the non-catalysed approach was used for the imprinting experiments.

Molecular imprinting with glass stamps

Glass stamp preparation

40 µL of a 200 ppm dilution of the respective nanoparticle suspension in distilled water was pipetted onto APTES-modified glass plates. Before application, the nanoparticle suspension was treated in the sonication bath for at least ten minutes to avoid aggregation of the nanoparticles. The stamps were placed in the drying cabinet at 80°C to evaporate the solvent. The dry stamps were first rinsed with acetone and afterwards with distilled water. Before use they were dried.

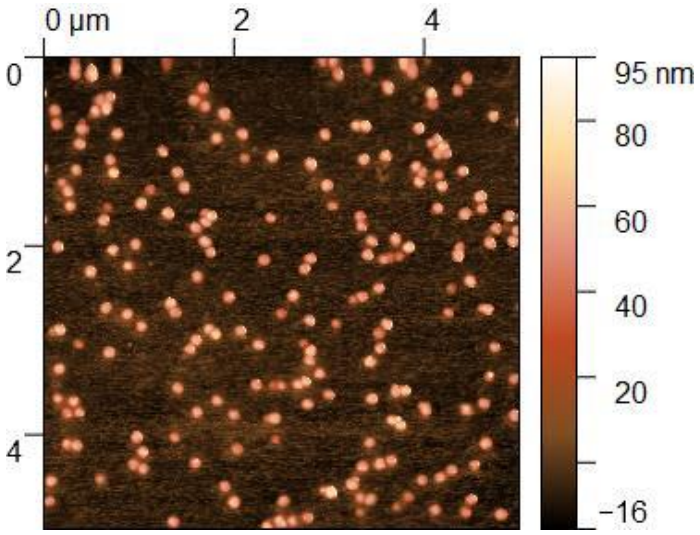

Figure 43: Glass stamp with 75 nm Ag NP

Figure 43 shows an AFM image of a nanoparticle stamp prepared with 75 nm silver nanoparticles. The nanoparticles are distributed all over the glass surface. However, some of the particles form small aggregates.

Amine blocking on glass stamps

The first protecting group tested was acetaldehyde. The nanoparticle stamps were placed in a petri dish containing 1 mL acetaldehyde in 20 mL dichloromethane. It was stirred for 1h at room temperature. Afterwards, the stamps were rinsed with dichloromethane and dried.

Another approach comprised of 1 mL acetic anhydride in 20 mL ethyl acetate. The stamps were stirred in this mixture at room temperature for one hour, rinsed with ethyl acetate, and dried.

Imprinting with glass stamps

Non-catalysed polyurethane (1:5 dilution in THF) served for imprinting. It was spin coated on APTES modified glass plates for 60 sec at 2000 rpm. The glass plate was placed on a microscope slide and the stamp was pressed on the polymer surface with the nanoparticles facing downwards. Another microscope slide was placed on top of the stamp and secured with clamps; the samples were cured overnight at 80°C.

For each batch of amine-protected stamps we prepared control stamps without the respective protecting group and used them for imprinting in the same way. The glass stamps could be removed without problems. However, also the control stamps did not stick to the polymer significantly.

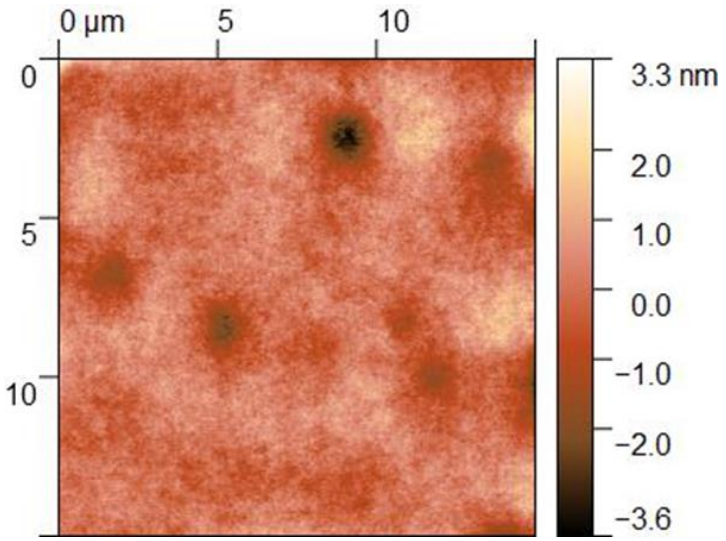

Figure 44: PU after imprinting with glass stamps 20x20 µm

The polyurethane surface was analysed by AFM to characterise nanoparticle imprints, if present. Figure 44 shows an AFM image of a PU surface after imprinting recorded with a scan size of 20 µm. This scan size is too large to find individual imprints but gives an overview of

the surface. It is very smooth, which is also reflected in the height scale bar on the right-hand side. It shows that the sample has a surface roughness of around 3 nm. Sometimes the polymer formed pores. However, they did not cover the whole surface, like in the case of catalysed PU.

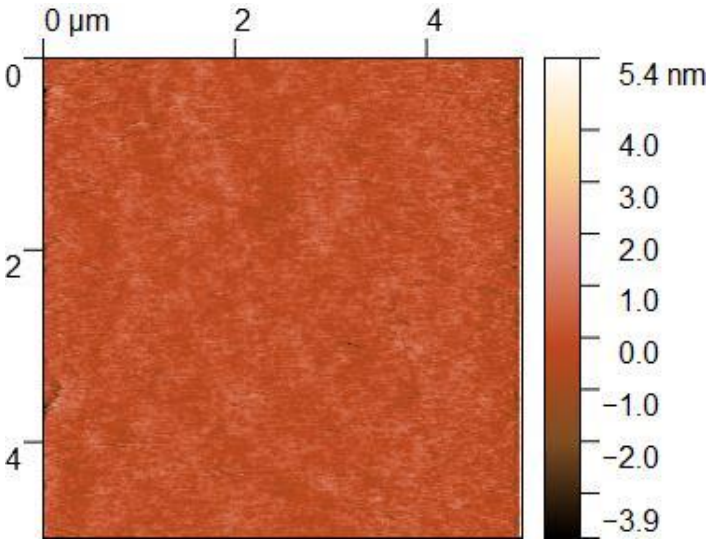

Figure 45: PU after imprinting with glass stamps 5x5 µm

Figure 45 shows a smaller fraction of PU surface after imprinting. A scan size of 5 µm is ideal to find imprints of the nanoparticles on the surface. However, as the AFM image shows, the surface is completely flat and lacks any visible imprints. All samples prepared with glass stamps looked like the two examples above. It did not make any difference if stamps without protection group or stamps treated with acetaldehyde or acetic anhydride were used. The experiments were repeated several times with NPs of both sizes. No imprints were visible on any sample.

Glass stamp imprinting: optimization

Having not found any nanoparticle imprints led us to assuming that the polymer layer had become already too hard after spin coating. This could also explain why the stamps without protecting group did not stick to the substrates in these experiments. Several parameters were varied one by one to obtain softer polymer layers after spin coating. For optimisation we used only stamps comprising nanoparticles with diameter d=75 nm and acetaldehyde as the protective group. For all experiments, we prepared control stamps without protecting group and used them in the same way as the protected ones.

Dilution

The dilution factor used for spin coating may be one parameter influencing the properties of the polymer layer. This influence was tested by using different dilutions of the pre-polymer:

Instead of 1:5, the pre-polymer solution was diluted 1:3, 1:8, 1:10 and 1:20 before spin coating. None of these batches led to imprints in the polymer.

Spin coating parameters

Spin coating time is a significant parameter. During spin coating the pre-polymer spreads on the surface to form a thin layer. During this process the solvent evaporates very quickly. This means that the polymer hardens quickly. The longer the sample is spun, the more solvent can evaporate. The original spin coating time of 60 seconds was shortened to 40 seconds and 20 seconds respectively.

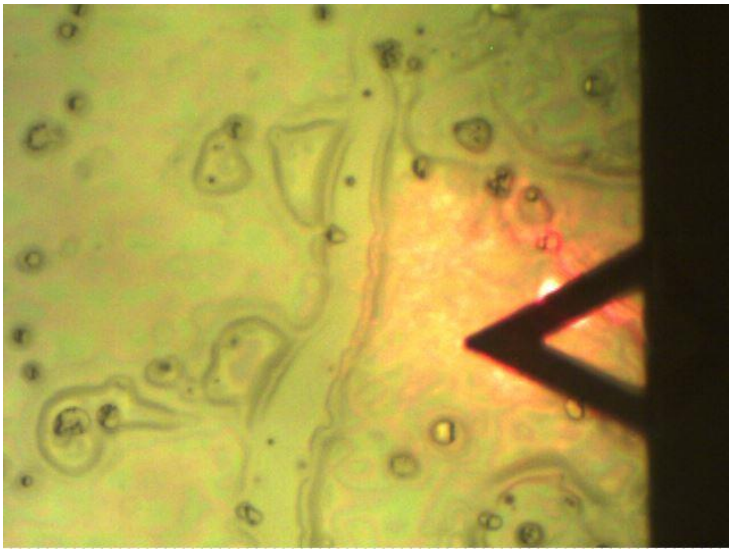

Figure 46: PU after 20 sec spin coating; light microscope image with AFM cantilever

These adjustments did not improve results. Shorter spin coating, especially for only 20 seconds led to inhomogeneous spreading of the polymer layer. This is visible in Figure 46.

Pre-polymerisation time

Another reason for a hard polymer could have been the long pre-polymerisation time. The shorter pre-polymerisation time, the smaller and less cross-linked the polymer chains are, when they are spin coated. The original pre-polymerisation time was 3 h and 20 min. It was shortened to 2 h 40 min and 2 h respectively. The pre-polymer was spin coated for 60 seconds at 2000 rpm. These changes did not lead to nanoparticle imprints.

Drop coating

Some samples were prepared by drop coating the pre-polymer solution onto the glass plates instead of spin coating. Here the problem of a cured polymer before imprinting would not occur because the polymer is applied as a solution and is cured when the stamp is already applied. When the polymer layer is drop coated the layer height can be controlled by the amount of solution used.

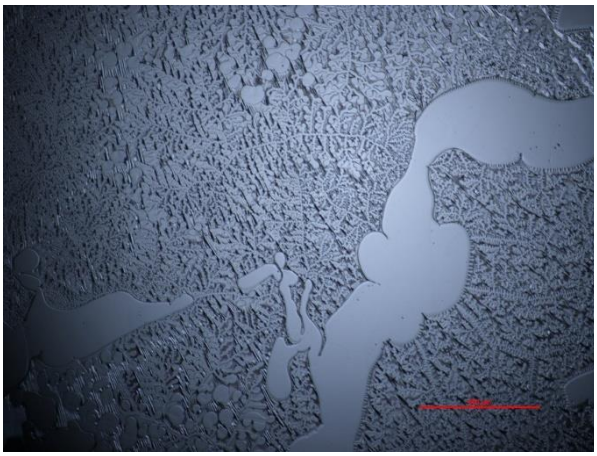

Figure 47: Drop coated PU surface after imprinting

Figure 48: Stamp after imprinting drop coated PU

Above light microscope pictures of the polymer surface (Figure 47) as well as the stamp (Figure 48) of a drop coated sample can be seen. The stamps were sticking to the polymer and could only be removed when force was applied. Some stamps were impossible to remove at all. In the microscope it was evident that parts of the polymer layer were ripped off during stamp removal leaving behind a pattern of polymer on the glass. On the stamps the same pattern of polymer could be observed.

Solvent

As none of the modifications mentioned above led to any improvement, the solvent THF was exchanged for a less volatile one. As already mentioned above, during spin coating the solvent evaporates rapidly. When a less volatile solvent is used at the same conditions, less of it is evaporated and the polymer is softer after spin coating.

Different solvents for polyurethane synthesis were tested. Toluene, p-xylene and ethyl acetate were not suitable since the solution turned turbid during pre-polymerisation. With dimethyl sulfoxide (DMSO) the solution remained clear. However, after spin coating small drops were visible on the glass slide suggesting that the polymer did not spread to form a layer.

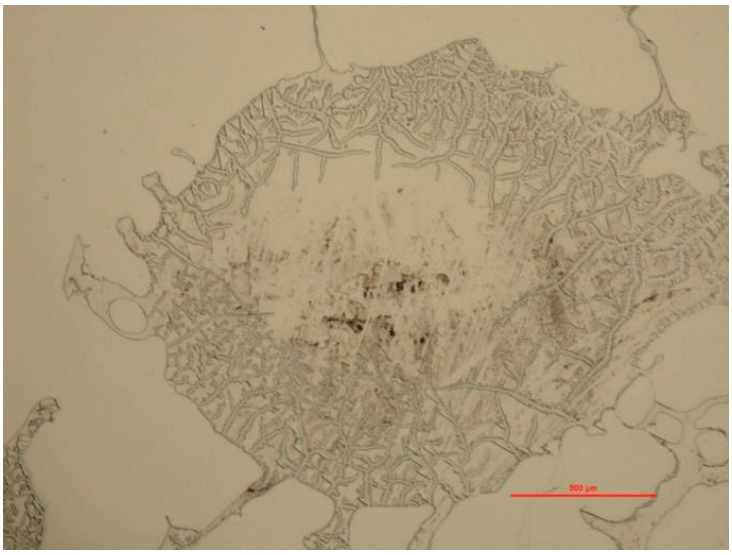

Figure 49: MIP PU film prepared with DMSO under the light microscope

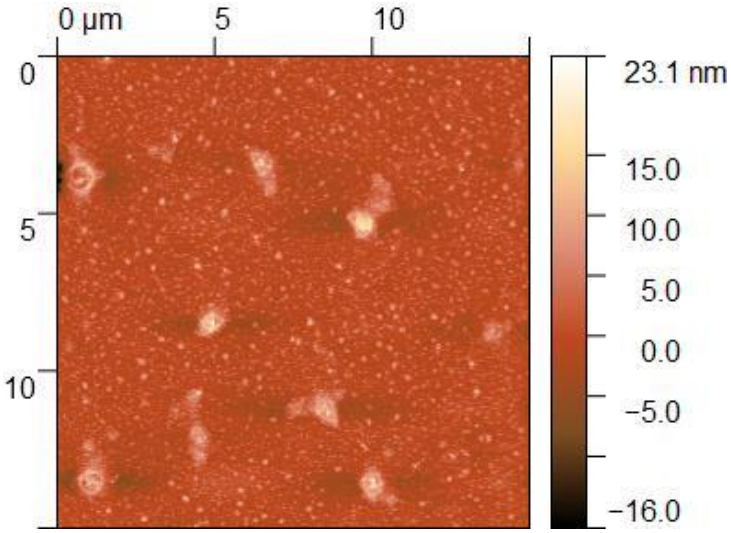

Figure 50: MIP PU prepared with DMSO

The stamps were harder to remove than with the initial polymer. After stamp removal the polymer surface was very rough and inhomogeneous. Images of the polymer in the light microscope (Figure 49) and in the AFM (Figure 50) can be seen above. The light microscope image suggests that parts of the polymer were ripped off with the stamp. It is also visible that the polymer is not spread on the whole surface.

Poly(styrene-co-divinylbenzene)

The glass stamps were tested on a different polymer to check whether the stamps or the polymer caused the problem. For spin coating poly(styrene-co-divinylbenzene) on glass the glass plates had to be modified in advance. They were cleaned in acetone in the sonication

bath for 5 minutes. Then they were treated in the plasma discharger for 5 min. The glass plates were placed in a petri dish with 400 µL 3-(methacryloyloxy)propyltrimethoxysilane in 20 mL toluene for 1 h and 30 min. They were rinsed with toluene, ethanol and water in that order and dried. 250 µL styrene and 250 µL divinylbenzene were mixed in an Eppendorf tube. 9 mg 2,2'-azobis(2-methylpropionitrile) (AIBN) were added and mixed well. The tube was placed in a water bath at 70°C for approximately 30 min until the mixture reached the gel point. 20 µL of the pre-polymer was spin coated on the modified glass plates at 2000 rpm for 10 seconds. Then Ag NP glass stamps without protecting groups were pressed into the polymer layer and secured between two microscope slides with clamps. The polymer was cured at 80°C overnight.

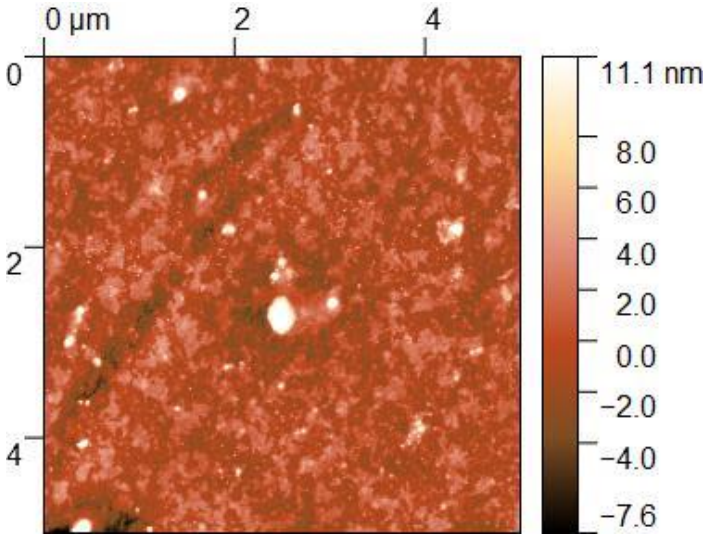

Figure 51: Poly(styrene-co-divinylbenzene) after imprinting with Ag NP glass stamps

In the AFM image of one of the samples (Figure 51) it is visible that the stamps did not leave behind any imprints. Since no imprints were obtained with glass stamps regardless of all optimisation steps the assumption was made that glass stamps are not suitable for this task. The fact that it was also impossible to imprint a different polymer than PU strengthens this hypothesis.

Molecular imprinting with PDMS stamps

PDMS stamp preparation

PDMS was prepared using the elastomer kit. The silicon elastomer and the curing agent were mixed in a mass ratio of 9:1. The mixture was degassed in a vacuum desiccator. Then it was poured into plastic petri dishes. The cured PDMS was cut into rectangular pieces and treated in the plasma discharger for 5 seconds. Longer plasma treatments cause cracks in the PDMS surface. Afterwards 20 µL of a solution of 10% APTES in ethanol was applied for 5 min. The stamps were rinsed with ethanol and water. 40 µL of a 100 ppm suspension of the silver

nanoparticles were applied and the stamps were dried in the oven at 80°C for 1 h. An AFM image of a PDMS stamp with 75 nm NPs is shown in Figure 52.

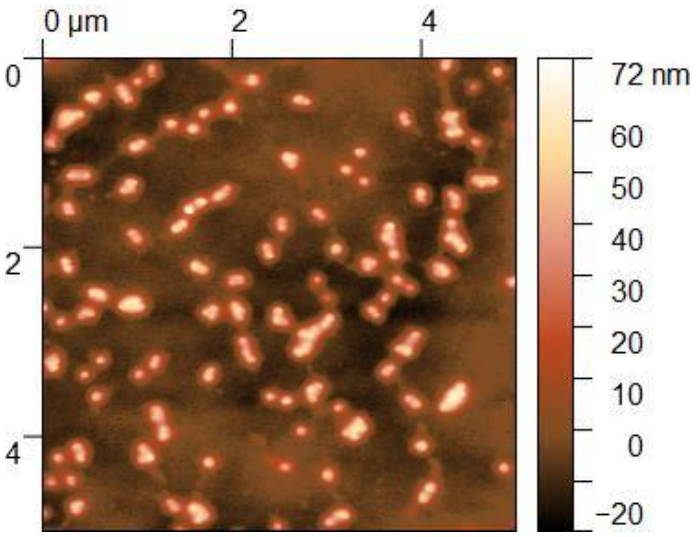

Figure 52: PDMS stamp with 75 nm Ag NP

Amine blocking on PDMS stamps

In the same way as in the case of the glass stamps, acetic anhydride and acetaldehyde were tested as protecting groups for the amines on the PDMS stamps. 40 µL of the respective reagent were applied on the dry stamps for 2 h. Afterwards the remaining fluid was removed and the stamps were dried in the oven. Control stamps were prepared in the same way without the protecting groups and used in the experiments to verify the results.

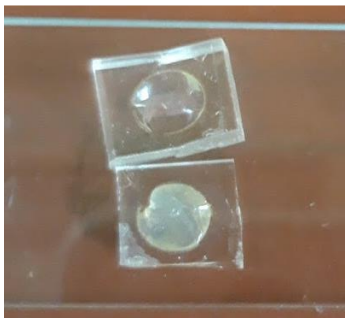

Figure 53: PU and PDMS stamp treated with acetaldehyde after imprinting

The control stamps were sticking to the polymer surface. It thus was impossible to remove them. The stamps prepared with acetaldehyde were sticking as well and not removable: When trying this, the PDMS located above the nanoparticles broke and stuck to the polymer (as can

be seen in the sample shown in Figure 53). On the bottom of the picture there is the polymer coated glass. The surface reveals a golden hue. That comes from the nanoparticles and parts of the PDMS sticking to the polymer. The PDMS stamp on the top of the picture has a hole in the middle where the PDMS was ripped off.

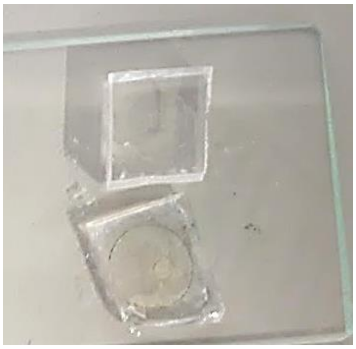

Figure 54: PU and stamp treated with acetic anhydride after imprinting

Stamps prepared with acetic anhydride could be removed without breaking the stamp (Figure 54). However, the nanoparticles were transferred onto the polymer. On the glass slide with the polymer (on the bottom of the picture) one can see the golden colour of the nanoparticles. The stamp, however, looks completely empty. That shows that most of the nanoparticles were transferred onto the polymer during imprinting.

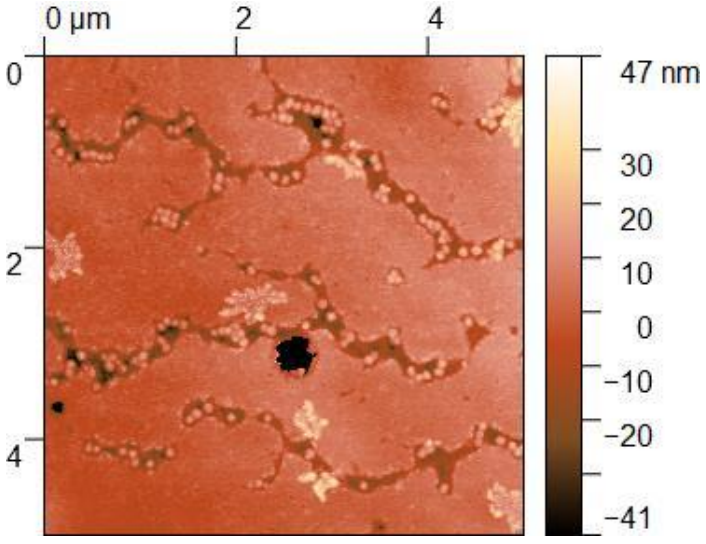

Figure 55: PU after imprinting with a PDMS stamp treated with acetic anhydride after 48 h washing

The MIP samples were washed in 10% acetic acid and 1% sodium dodecyl sulfate (SDS) in deionised water to remove the particles. After 48 h the polymer surface was analysed in the AFM and resulted in the image of the surface shown in Figure 55. The nanoparticles are visible and seem to be embedded in groves in the polymer. The exact reasons for this behaviour are yet unclear.

Peak force measurement

Since the nanoparticles are evenly distributed on the surface of the stamps, this should also be the case on the polymer. The fact that there are areas without particles and imprints in between the valleys, raised suspicions that the particles could be covered by a polymer layer. This was further examined by peak force tapping AFM measurements.

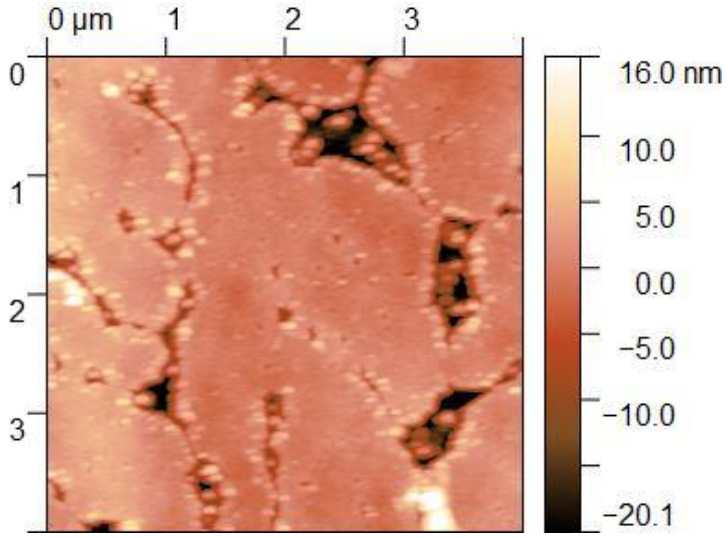

Figure 56: Peak force measurement: height image

Figure 56 shows the height image. It looks similar to the ones shown previously. The sample was washed for 24 h in 10% acetic acid and 1% SDS prior to analysis. Nanoparticles are visible in voids in the layer.

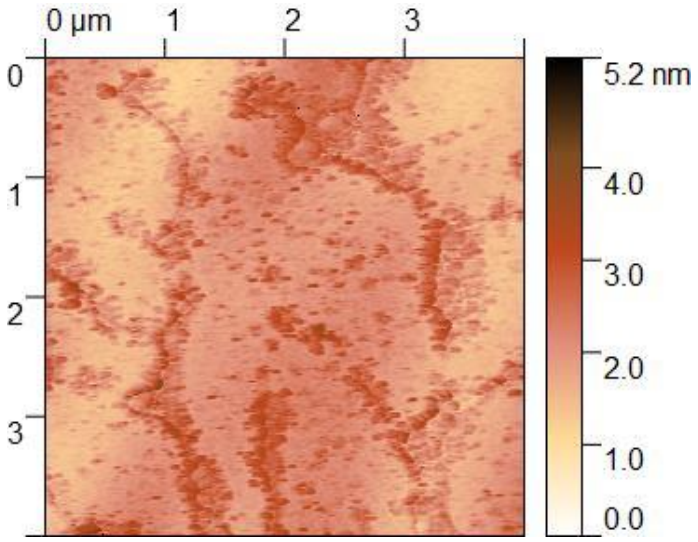

Figure 57: Peak force measurement: deformation image

Figure 57 shows the deformation image of the same measurement. The maximum deformation is defined as the penetration of the tip into the sample surface at peak force. The areas, where nanoparticles are visible in the height image show more deformation than the flat surfaces. Also, circular structures with higher deformation that were not visible in the height images showed up on the flat surface. These results suggest that the nanoparticles are in fact buried under a polymer layer. However, due to the limited number of results no definitive statement can be made at the present moment. How these surfaces formed and why they only occur on some of the samples even though the procedure is not changed requires further investigations. The peak force measurement was only performed once with one sample. The scope was to check if there would be any difference to the height images. Since the formation of these structures was not part of the main issues addressed in this project it was not further examined.

PDMS stamp imprinting: optimisation

Since the nanoparticles were transferred onto the polymer and could not be washed out, the next step aimed at modifying polymer synthesis and deposition to decrease layer height. The idea behind this was that the nanoparticles would not sink in as deep as in thicker layers and thus could be washed out of the cavities.

Decreasing layer height by spin coating

To achieve this, in the first step the pre-polymer solution was diluted 1:10 and 1:20 instead of 1:5 before spin coating. In the second step the spin coating parameters were changed. Velocity was increased to 2500 rpm and 3000 rpm. The spin coating time of 60 sec was not changed.

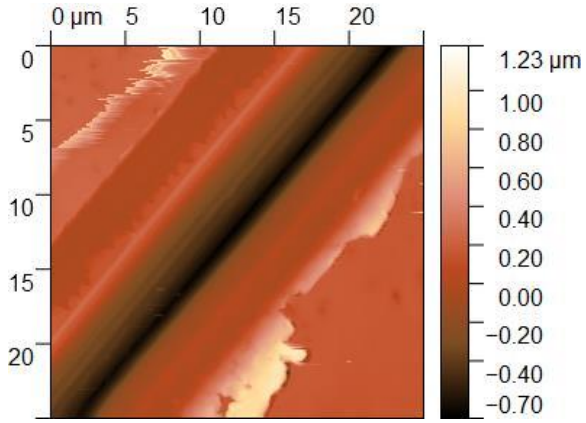

Figure 58: AFM image of a cut in PU

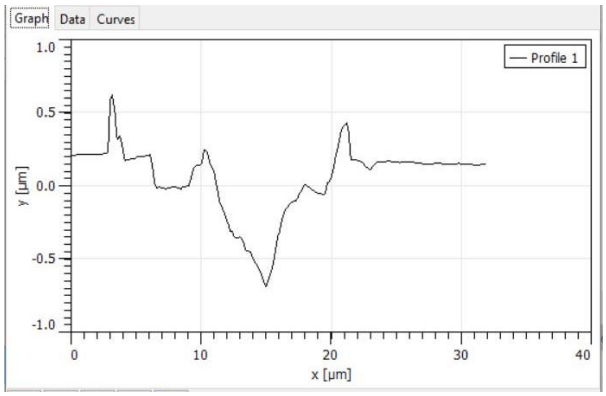

Figure 59: Profile of a cut in PU

The layer height was determined by cutting the polymer layer and taking an AFM image of the cut and the adjacent polymer surface. Figure 58 and Figure 59 contain images from the outcome of this procedure. It was possible to determine layer height by measuring the difference between the flat polymer and the deepest point in the cut. This method is not very reliable or reproducible, but it gives an idea of the dimensions of the layers. The aim was to produce layers that are sufficiently thin for washing out the nanoparticles even if they sink into the polymer.

Table 3: Layer heights of PU samples prepared with different dilutions and spin coating velocities

Spin coating (60 s)	**1:5**	**1:10**	**1:20**
2000 rpm	890 nm	230 nm	40 nm
2500 rpm	250 nm	60 nm	60 nm
3000 rpm	220 nm	60 nm	50 nm

Table 3 summarises the results of the layer height determination of the spin coated samples. As expected, the layer height decreases with decreasing polymer concentration and increasing spin coating velocity. It seems like the minimum is reached at around 60 nm. All polymers described in the table above were prepared and imprinted with PDMS stamps treated with acetic anhydride.

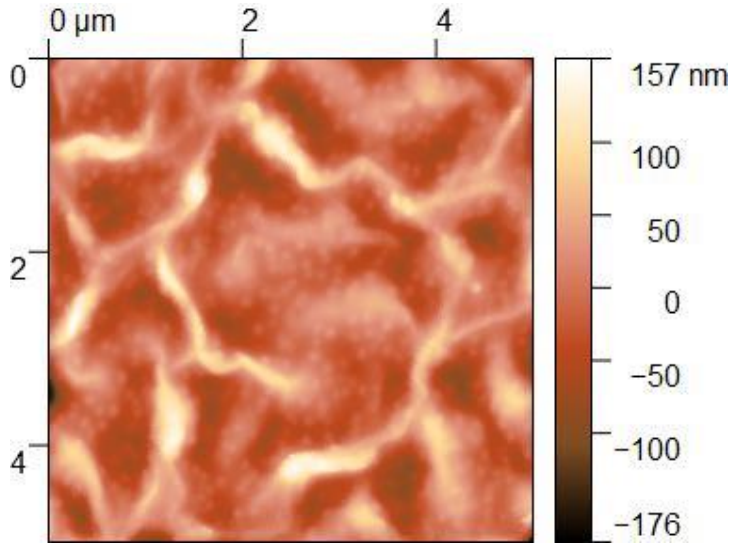

Figure 60: Wrinkles on a PU sample; 1:10 dilution spin coated with 2500 rpm

Layers prepared with the more diluted polymers tended to form wrinkled surfaces which is demonstrated in Figure 60. Sometimes the wrinkles were also observed in the samples prepared with polymer solutions containing higher concentrations. These structures may be caused by the PDMS stamps. The oxidised surface of the elastomer can form wrinkles due to expansion and subsequent contraction when the material experiences high temperatures and cools down again during stamp preparation. [40]

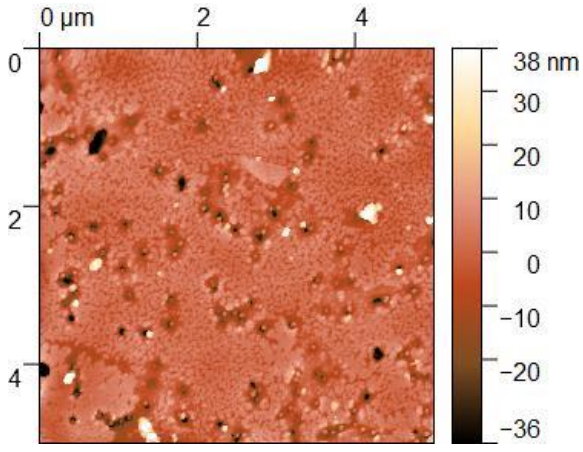

Figure 61: PU MIP (1:10, 3000 rpm) after washing

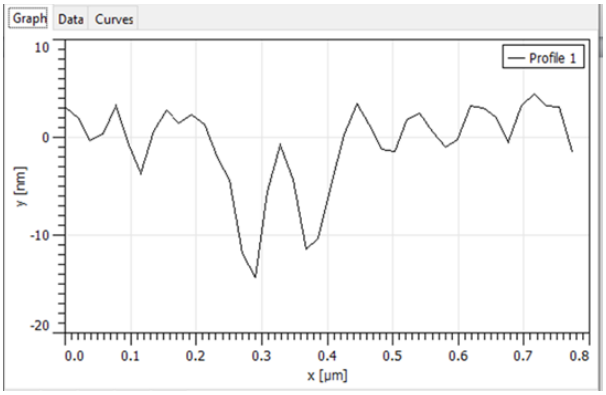

Figure 62: Profile of a nanoparticle stuck in PU

Figure 61 shows a PU sample after imprinting. A 1:10 dilution was spin coated onto glass with 3000 rpm. One can clearly see on this image that the nanoparticles sink into the polymer layer. The image was taken after 24h washing in 10% acetic acid and 1% SDS in water. Some cavities were empty, but most nanoparticles remained in the matrix.

Figure 62 is a height profile of a section of the previous AFM image. It shows a nanoparticle stuck in a cavity in the polymer. This shows that the nanoparticles are sinking into the polymer. The highest point of the NPs is on the same level as the polymer surface. For successful removal at least half of the particle should be above the PU layer.

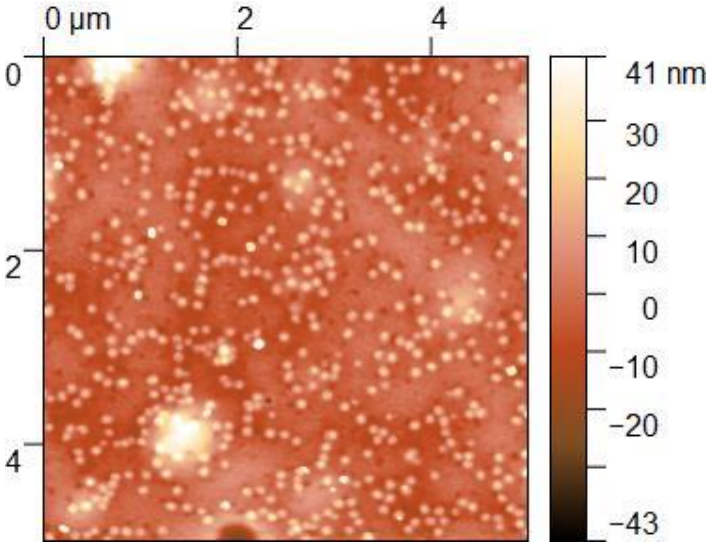

Figure 63: MIP PU (1:10, 2000 rpm) after washing for 24h

In other samples like the one in Figure 63, nanoparticles did not sink in as deep. Still it was impossible to remove them from the polymer. This suggests strong affinity between the particles and the polymer.

Further optimisation

Another approach included imprinting without applying pressure. The samples were prepared as usual. After the stamp was placed on the polymer layer, no pressure was applied with clamps. The polymer was cured at 80°C.

To avoid that the nanoparticles were pulled into the polymer by gravity, samples were imprinted "upside-down" This means that the stamp was placed on the bench with the nanoparticles facing upwards. The polymer was spin coated onto the glass slide as usual. Then the glass was inverted and placed on the stamp with the polymer layer facing downwards. Pressure was applied with clamps and microscope slides and the polymer was cured at 80°C.

Both attempts did not change the results. The nanoparticles were embedded in the polymer. Washing in 10% acetic acid and 1% SDS could not remove the particles.

Decreasing layer height by drop coating

Samples were prepared from drop coated polyurethane. The height of drop coated layers can be controlled by the amount of oligomer solution applied. The smaller the volume of

pre-polymer solution applied, the thinner the layer is. Various volumes of the different dilutions were tested.

Table 4: Summary of the results of the layer height determination of the drop coated samples

Drop coating	5 µL	4 µL	3 µL	2µL
1:5	1 µm	1.7 µm	1 µm	479 nm
1:10	-	-	160 nm	80 nm
1:20	-	-	-	60 nm

The layer height was determined in the same way as with the spin coated samples. The layer heights of the drop coated samples are summarised in Table 4. Layers prepared with the 1:5 diluted PU were too thick. The heights of layers prepared with a small amount of the more diluted polymers were in the desired range.

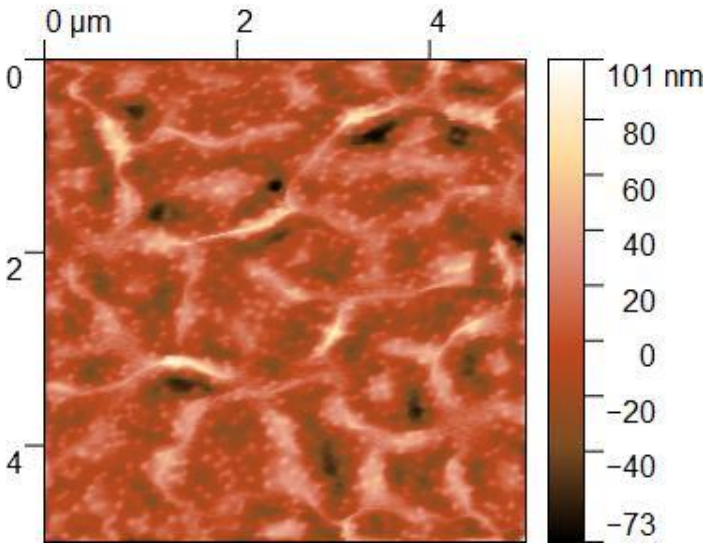

Figure 64: MIP PU after washing prepared by drop coating (2 µL, 1:10)

However, it was not possible to wash the nanoparticles out of the polymer. Figure 64 shows a sample prepared by drop coating 2 µL of the 1:10 dilution and imprinting it with PDMS NP stamps. After extensive washing the surface is still completely covered with the nanoparticles.

Template removal

In all experiments with the PDMS stamps treated with acetic anhydride the nanoparticles were transferred onto the polymer layer. A washing solution containing 10% acetic acid and 1% SDS in water was used to wash them out of the cavities. This washing solution has been frequently used in the group to remove a range of different templates. Stirring the samples in the washing solution for up to 48 h did not lead to visible removal of nanoparticles.

A different approach aiming at dissolving the silver was chosen. Nitric acid (HNO_3) is known for its ability to dissolve metals, including silver. A 1:3 dilution of HNO_3 was used to remove the nanoparticles from the polymer.

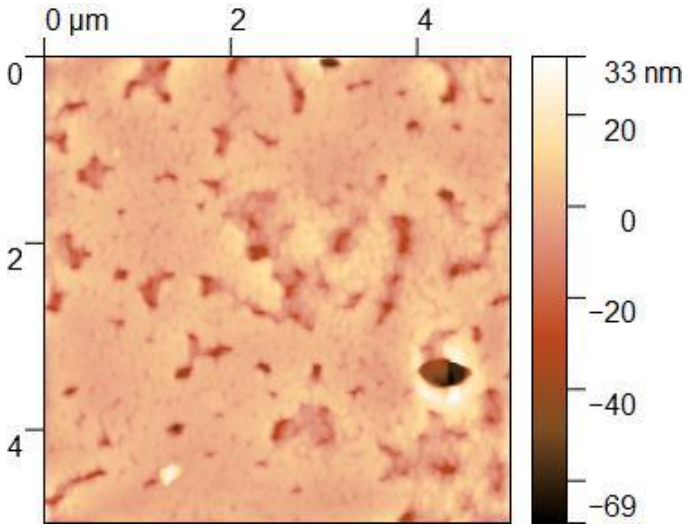

Figure 65: MIP after 2.5h in HNO3 (1:3)

The sample shown in Figure 65 was immersed in a 1:3 dilution of HNO_3 (3,6 mol/L) for 2.5 h. A complete removal of the nanoparticles was not possible. However, better results than with the washing solution were obtained. As the picture above shows, all cavities on this 5x5 µm scan are empty. Comparable results were never reached when the samples were stirred in the washing solution. However, this possibility was not extensively explored in this project. Further experiments are necessary to fully confirm the results and potentially achieve complete template removal.

Poly(styrene-co-divinylbenzene)

The PDMS stamps were tested on poly(styrene-co-divinylbenzene) as well. The polymer was prepared in the same way as described in the glass stamp section. For imprinting PDMS stamps without protecting group and stamps treated with acetic anhydride were used. The aim was to obtain information about the effect on the stamps caused by the acetic anhydride treatment.

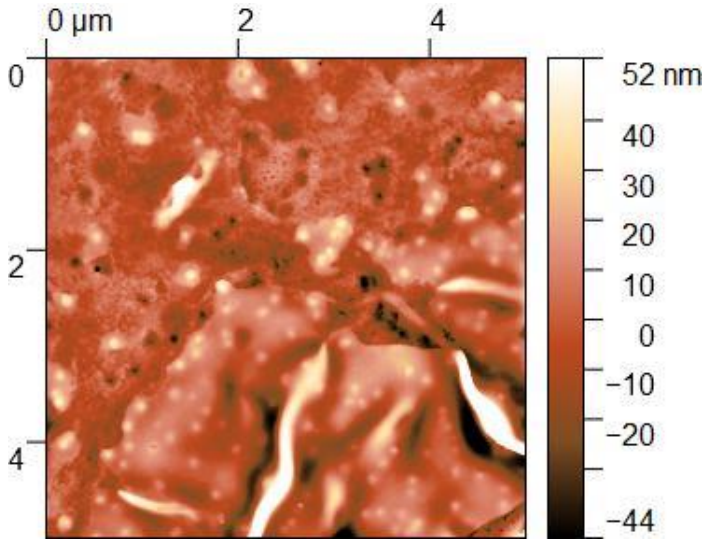

Figure 66: Poly(styrene-co-divinylbenzene) imprinted with PDMS stamps treated with acetic anhydride

Figure 66 shows the surface of a sample imprinted with a stamp treated with acetic anhydride. The sample was rinsed with distilled water after stamp removal, but not washed in any washing solution. In the same way as during experiments with PU, the nanoparticles detached from the PDMS stamp. Some empty imprints are visible on the unwashed samples, which is different from PU samples: in that polymer, usually all cavities are still occupied by NPs even after extensive washing. This might suggest that the nanoparticles have lower affinity to poly(styrene-co-divinylbenzene), than to polyurethane.

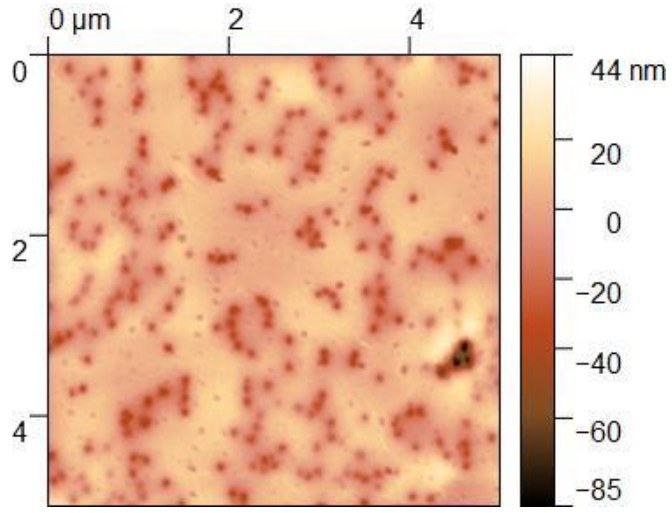

Figure 67: Poly(styrene-co-divinylbenzene) imprinted with PDMS stamps without protecting group

When stamps without protecting groups were used, the nanoparticles stayed on the PDMS stamps. The stamps were easily removable, which confirms that the problem of adhering

stamps is tied to the use of polyurethane. The AFM image of the imprinted sample surface (Figure 67) was taken immediately after stamp removal and brief rinsing with distilled water. No washing was necessary. The surface is covered with imprints of the nanoparticles. No embedded nanoparticles were visible on the polymer.

Acetic anhydride is necessary to prevent the APTES-modified stamps from sticking to the polyurethane surface. However, the results obtained with poly(styrene-co-divinylbenzene) suggest that the use of acetic anhydride causes another problem, namely transfer of the NPs from the stamps into the polymer layer. A possible reason is that the anhydride weakens the interaction between APTES and the nanoparticles. Acetic anhydride reacts with the primary amine groups in the APTES. The nanoparticles adsorb on APTES by electrostatic interactions. If the anhydride does not only react with the remaining amine groups, but also those which interact with the NPs, the forces which hold the NPs on the stamp are significantly decreased. Consequently, NPs detach from the PDMS stamp and sink into the polymer as soon as the stamp is applied. In addition, the NPs seem to have high affinity towards PU which makes it impossible to remove them, once they are embedded in the polymer layer.

Alternative ways of nanoparticle immobilisation

To overcome the problems caused by APTES on PDMS stamps, alternative ways for immobilising the NPs were explored. Since the nanoparticles seemed to be highly affine to polyurethane, this polymer was tested as an adhesive on the stamps. PDMS stamps were prepared as usual and treated with acetic anhydride. Those stamps were used for transferring the nanoparticles. A small amount (1 or 2 µL) of a 1:20 dilution of the polyurethane formulation usually used for the MIPs was drop coated on APTES modified PDMS stamps. A PDMS NP stamp treated with acetic anhydride was placed on the pre-polymer. Pressure was applied with microscope slides held together by clamps and the polymer was cured at 80°C overnight.

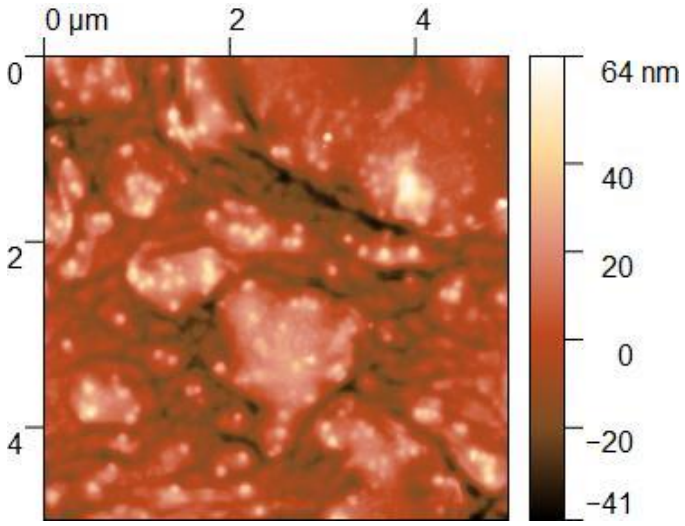

Figure 68: NPs immobilised on PU on PDMS (2 µL 1:20 PU)

As expected, the nanoparticles were transferred onto the polymer. An AFM image of a stamp prepared with 2 µL of a 1:20 dilution is depicted in Figure 68. The nanoparticles are protruding from the surface. However, the polymer surface is irregular and rough, which is not ideal for imprinting. Imprinting on PU is impossible with these stamps. Since the same polymer is used on both the stamp and the substrate, the polymer layers stick together. Some stamps were tested on poly(styrene-co-divinylbenzene). They could be removed without any problems. However, no imprints were found on the polymer samples.

This idea occurred towards the end of the project and was not extensively explored. Further experiments are necessary to clarify if stamps with nanoparticles immobilised in PU can be prepared and used for imprinting.

6. Conclusions and outlook

Humidity experiments revealed that humid conditions during polymer curing are related to surface porosity of polyurethanes synthesised without using a catalyst: high humidity leads to pores appearing on the surface. At dry or normal conditions, PU surfaces are usually smooth and form hardly any visible pores. This means that maintaining a dry atmosphere is beneficial when polyurethane thin films are prepared following this route. In contrast, samples prepared via catalysed polyaddition did not show any correlation between pore formation and humidity: Both samples cured in dry and humid conditions revealed large circular structures, while the control sample had a porous surface.

Optimising the catalysed polyaddition did not significantly improve surface topography. Most approaches did not reduce pore formation. The only correlation found was related to catalyst concentration: Using very small amounts of the catalyst seemed to decrease pore density on the surface. However, decreasing the catalyst concentration also decreases the positive effects of the catalyst, such as shorter reaction times. In addition, thin films prepared with small catalyst concentrations were very inhomogeneous. Formation of pores could not be completely avoided. Thus, the present project could not obtain satisfactory results in that regard. To clarify the origin of the pores and prove any possible connection to catalyst concentration, more experiments are necessary, which was not possible in this project due to time constraints.

Molecular imprinting of polyurethane thin films with silver nanoparticles immobilised on glass stamps was not successful. Template stamps which previously were impossible to remove from the polymer after imprinting did not adhere to the polymer in these experiments. Acetaldehyde and acetic anhydride were tested as protecting groups. Neither modified nor control stamps adhered to the polymer surface. This made it impossible to determine whether the protecting groups worked or not. Unfortunately, no imprints were detected in PU, regardless of the modification of stamps. No cavities were visible on poly(styrene-co-divinylbenzene) imprinted with glass stamps without protecting groups. This leads to the conclusion that glass stamps may not be suitable for imprinting nanoparticles. Further experiments, especially with other polymers are necessary to verify this hypothesis.

PDMS NP stamps stuck to the polyurethane surface due to the APTES modification. This issue could be solved by treating the stamps with acetic anhydride. The stamps could be removed without breaking. However, the nanoparticles were detached from the PDMS and were transferred into the polymer layer. The nanoparticles could not be removed by extensive washing. Decreasing the layer height did not improve things. Template removal by dissolving the nanoparticles in nitric acid led to better results. However, it turned out impossible to completely remove all nanoparticles.

Imprinting poly(styrene-co-divinylbenzene) with PDMS stamps indicated that acetic anhydride may be responsible for the detachment of the nanoparticles from the PDMS. Samples imprinted with stamps modified with acetic anhydride looked similar to PU samples. The nanoparticles were “stuck” in the polymer. When unmodified stamps were used, this problem did not occur: nanoparticles remained on the stamp after imprinting and stamp removal. The surface was covered with imprints. No washing was necessary. A possible explanation is that acetic anhydride competes with the nanoparticles for APTES molecules. Thus, the interaction between nanoparticles and APTES is weakened. This means that acetic anhydride is probably not the ideal protecting group for this application. Other protecting groups should be explored. However, the results suggest that PDMS is better suited for imprinting with silver nanoparticles. This could be explained by the flexibility of the material. The elastomer can get into better contact with the polymer surface than the rigid glass stamps.

Other methods of immobilising the nanoparticles on PDMS without using APTES were explored. The nanoparticles could be successfully immobilised in polyurethane. However, the stamps could not be used for imprinting. Those stamps adhered to polyurethane. On poly(styrene-co-divinylbenzene) they did not produce imprints. This part was only briefly touched upon towards the end of the project and needs more research and experiments before a definitive statement can be made.

7. References

[1] O. Bayer, „Das Di-lsocyanat-Polyadditionsverfahren (Polyurethane),“ *Angewandte Chemie,* pp. 257-288, 1947.

[2] J. O. Akindoyo, M. D. H. Beg, S. Ghazali, M. R. Islam, N. Jeyaratnama und A. R. Yuvarajc, „Polyurethane types, synthesis and applications – a reviw,“ *RSC Advances,* p. 114453, 2016.

[3] K. M. Zia, S. Anjum, M. Zuber, M. Mujahid und T. Jamil, „Synthesis and molecular characterization of chitosan based polyurethane elastomers using aromatic diisocyanate,“ *International Journal of Biological Macromolecules,* pp. 26-32, 2014.

[4] K. Haupt, in *Molecular Imprinting*, Berlin, Springer, 2012.

[5] M. Charlon, B. Heinrich, Y. Matter, E. Couzigné, B. Donniocd und L. Avérousa, „Synthesis, structure and properties of fully biobased thermoplastic polyurethanes, obtained from a diisocyanate based on modified dimer fatty acids, and different renewable diols,“ *European Polymer Journal,* pp. 197-205, 2014.

[6] N. N. P. N. Pauzi, R. A. Majid, M. H. Dzulkifli und M. Y. Yahya, „Development of rigid bio-based polyurethane foam reinforced with nanoclay,“ *Composites Part B: Engineering,* pp. 521-526.

[7] P. Alagi, Y. J. Choi und S. C. Hong, „Preparation of vegetable oil-based polyols with controlled hydroxyl functionalities for thermoplastic polyurethane,“ *European Polymer Journal,* pp. 46-60, 2016.

[8] R. Arshady und K. Mosbach, „Synthesis of substrate-selective polymers by host-guest polymerization,“ *Makromol. Chem.,* pp. 687-692, Jänner 1981.

[9] G. Wulff und A. Sarhan, „The use of polymers with enzyme-analogous structures for the resolution of racemates,“ *Angew. Chem. Int. Ed.,* p. 341, 1972.

[10] L. Chen, X. Wang, W. Lu, X. Wua und J. Lia, „Molecular imprinting: perspectives and applications,“ *Chemical Society Reviews,* pp. 2137-2211, 2016.

[11] D. R. Kryscio und N. A. Peppas, „Critical Review and Perspective of Molecularly Imprinted Polymers,“ *Acta Biomateriala, 8,* pp. 461-473, 2012.

[12] D. Refaat, M. G. Aggour, A. A. F. R. Mahajan, J. G. Wiklander, I. A. Nicholls und S. A. Piletsky, „Strategies for Molecular Imprinting and the Evolution of MIP Nanoparticles as Plastic Antibodies - Synthesis and Applications,“ *International Journal of Molecular Science,* p. 6304, 2019.

[13] P. Lieberzeit, C. Jungmann und L. Schranzhofer, „Molecular Imprinting on the Nanoscale - Rapid detection of Ag Nanoparticles by QCM Sensors,“ *Procedia Engeneering,* pp. 236-239, 2014.

[14] M. F. Frasco, L. A. A. N. A. Truta, M. G. F. Sales und F. T. C. Moreira, „Imprinting Technology in Electrochemical Biomimetic Sensors,“ *Sensors,* 6 März 2017.

[15] E. Hood, „Nanotechnology: Looking As We Leap,“ *Environmental Health Perspectives,* pp. A740-A749, 2004.

[16] T. X. L. M. N. L. Andre Nel, „Toxic potential of Materials at the Nanolevel,“ *Science,* pp. 622-627, 3 Februar 2006.

[17] J. W. Alexander, „History of the medical use of silver," *Surgical Infections,* pp. 289-292, 2009.

[18] Bernd Nowack, „Nanosilver Revisited Downstream," *Science,* pp. 1054-1055, 2010.

[19] C. Zhang, Z. Hu und B. Deng, „Silver nanoparticles in aquatic environments: Physiochemical behavior and antimicrobial mechanisms," *Water Research,* pp. 403-427, 2016.

[20] D. Clevelanda, S. E. Longa, P. L. Pennington, E. Cooper, M. H. Fulton, G. I. Scott, T. Brewera, J. Davisa, E. J. Petersen und L. Wood, „Pilot estuarine mesocosm study on the environmental fate of Silver nanomaterials leached from consumer products," *Science of The Total Environment,* pp. 267-272, 2012.

[21] E. McGillicuddy, I. Murray, S. K. L. Morrison, A. Fogarty, M. Cormican, P. Dockery, M. Prendergast, N. Rowan und D. Morris, „Silver nanoparticlesin the environment: Sources, detection and ecotoxicology," *Science of the Total Environment,* pp. 231-246, 2017.

[22] S. A. Blaser, M. Scheringer, M. M. Leod und K. Hungerbühler, „Estimation of cumulative aquatic exposure and risk due to silver: Contribution of nano-functionalized plastics and textiles," *Science of the Toal Environment,* pp. 396-409, 2008.

[23] W. Zhang, B. Xiao und T. Fang, „Chemical transformation of silver nanoparticles in aquatic environments: Mechanism, morphology and toxicity," *Chemosphere,* pp. 324-334, 2018.

[24] R. Grillo, A. H. Rosa und L. F. Fraceto, „Engineered nanoparticles and organic matter: A review of the state-of-the-art," *Chemosphere,* pp. 608-619, 2015.

[25] A. l. o. o. D. Dwivedi, S. P. Dubey, M. Sillanpää, Y.-N. Kwon, C. Lee und R. S. Varma, „Fate of engineered nanoparticles: Implications in the environment," *Coordination Chemistry Reviews,* pp. 64-78, 2015.

[26] T. A. j. d. Souza, L. R. R. Souza und L. P. Franchi, „Silver nanoparticles: An integrated view of green synthesis methods, transformation in the environment, and toxicity," *Ecotoxicity and Environmental Safety,* pp. 691-700, 2019.

[27] K. Loza und M. Epple, „Silver nanoparticles in complex media: an easy procedure to discriminate between metallic silver naoparticles, reprecipitated silver chloride, and dissolved silver species," *RSC Advances,* pp. 24386-24391, 2018.

[28] L. Pinďáková, V. Kašpárková, K. Kejlová, M. Dvořáková, D. Krsekc, D. Jírová und L. Kašparová, „Behaviour of silver nanoparticles in simulated saliva and gastrointestinal fluids," *International Journal of Pharmaeutics,* pp. 12-20, 2017.

[29] J. H. Shannahan, R. Podila und J. M. Brown, „A hyperspectral and toxicological analysis of protein corona impact on silver nanoparticle properties, intracellular modifications, and macrophage activation," *International Journal of Nanomedicine ,* pp. 6509-6521, 2013.

[30] K. Kettler, C. Giannakou, W. H. d. Jong, A. J. Hendriks und P. Krystek, „Uptake of silver nanoparticles by monocytic THP-1 cells depends on particle size and presence of serum proteins," *Journal of Nanoparticle Research,* pp. 1-9, 2016.

[31] S. Mukherjee, D. Chowdhury, R. Kotcherlakota, S. Patra, V. B, M. P. Bhadra, B. Sreedhar und C. R. Patra, „Potential Theranostics Application of Bio-Synthesized Silver Nanoparticles (4-in-1 System)," *Theranostics,* pp. 316-335, 2014.

[32] J. Jiravova, K. B. Tomankova, M. Harvanova, L. Malina, J. Malohlava, L. Luhovad, A. Panaceke, B. Manisova und H. Kolarova, „The effect of silver nanoparticles and silver ions on mammalian and plant cells in vitro," *Food and Chemical Toxicology,* pp. 50-61, 2016.

[33] B. M. Angel, G. E. Batley, C. V.Jarolimek und N. J. Rogers, „The impact of size on the fate and toxicity of nanoparticulate silver in aquatic systems," *Chemosphere,* pp. 359-365, 2013.

[34] P. Eaton und P. West, Atomic Force Microscopy, New York: Oxford University Press, 2010.

[35] „Bruker," 17 Noverber 2020. [Online]. Available: https://www.bruker.com/products/surface-and-dimensional-analysis/atomic-force-microscopes/modes/modes/imaging-modes.html.

[36] D. Yongabi, M. Korshid, P. Losada-Perez, K. Eersels, O. Deschaumere, C. B. J. H. R. T. Jan D`Haen, M. Wübbenhorst und P. Wag, „Cell detection by surface imprinted polymers SIPs: A study to unravel the recognition mechanisms," *Sensors and Actuators B: Chemical,* pp. 907-917, 2018.

[37] L. Schranzhofer, *Polymer-based receptors for silver and zinc oxide nanoparticles: characterization and optimization,* Wien, 2015.

[38] C. Jungmann, *Chemosensors for the Detection of Engineered Nanoparticles using Molecularly Imprinted Polymers,* Wien, 2015.

[39] H. Gliemann, A. T. Almeida, D. F. S. Petri und T. Schimmel, „Nanostructure formation in polymer thin films," *Surface and Interface Analysis,* pp. 1-8, 2006.

[40] W. T. S. H. K. E. P. a. G. M. W. Ned Bowden, „The controlled formation of ordered, sinusoidal structures by plasma oxidation of an elastomeric polymer," *Applied Physics Letters,* 1999.

8. Illustrations

8.1. Figures

8.2. Tables

9. Appendix

9.1. Abstract in English

This work aims at addressing issues that have occurred in previous projects in the research group during nanoparticle imprinting. The thesis is divided into two parts. The first one deals with polyurethane surfaces: Catalysed polyaddition frequently led to pore formation on surfaces of thin films. Possible causes for this needed to be tested: Experiments showed that only catalyst-free polymerisation led to a correlation of thin film porosity and humidity. For the catalysed reaction no clear cause could be identified: There was only weak correlation between porosity and catalyst concentration. It turned out impossible to obtain thin films without pores when using a catalyst.

The second part focussed on optimizing stamps used for molecular imprinting with silver nanoparticles. Glass stamps and PDMS stamps were used. Both need to be modified with APTES to immobilise the nanoparticles. Amine groups of the silane react with isocyanate functionalities of the forming polymer thin film and bind the stamps to the polymer. Thus, stamp and MIP cannot be separated from each other. Hence, we considered using acetaldehyde and acetic anhydride as protecting groups. In this project the glass stamps did not stick, even without protecting group. This made it impossible to evaluate the influence of modifications on those stamps. Imprints could not be produced with glass stamps on neither polyurethane nor poly(styrene-co-divinylbenzene).

In contrast, PDMS stamps stuck to polyurethane. Stamps treated with acetic anhydride could be removed without problems. However, nanoparticles detached from the PDMS and stuck in the polymer. Extensive washing and synthesis of thinner polymer layers could not solve this issue. When treating the surface with diluted nitric acid to dissolve the particles, this led to better results. However, it was not possible to remove all nanoparticles from the polymer.

PDMS stamps were also tested on poly(styrene-co-divinylbenzene). Both stamps without protecting groups and those modified with acetic anhydride were tested. Nanoparticles detached from the modified stamps in the same way as in the case of polyurethane. Unmodified stamps could be removed together with the nanoparticles and thus left behind imprints without the need of washing. This suggests that acetic anhydride weakens the interaction between APTES and the nanoparticles.

The results listed above suggest that PDMS stamps are better suited for imprinting polymers with silver nanoparticles, than glass stamps. This is probably due to their flexibility which allows for better contact with the polymer surface. More experiments are necessary to verify the hypotheses proposed in this work.

9.2. Deutsche Zusammenfassung

In dieser Arbeit wurden Probleme, die in vorherigen Projekten dieser Arbeitsgruppe aufgetreten sind, behandelt. Ziel war es, die Auslöser für diese Probleme und im Idealfall Lösungen dafür zu finden. Die Arbeit ist in zwei Teile unterteilt. Der erste Teil befasst sich mit der Optimierung von Polyurethanoberflächen. Bei katalysierter Polyaddition wurde eine starke Porenbildung in den Dünnschichten beobachtet. In diesem Projekt wurden mögliche Auslöser für dieses Phänomen gesucht. Dabei konnte nur bei der unkatalysierten Reaktion ein Zusammenhang zwischen der Luftfeuchtigkeit und der Porenbildung festgestellt werden. Bei katalysierten Reaktionen ergab sich kein eindeutiger Auslöser für die Porenbildung. Es wurde lediglich ein schwacher Zusammenhang mit der Katalysatorkonzentration festgestellt. Es war im Rahmen dieses Projektes nicht möglich porenfreie Dünnschichten mit aus katalysierten Polymerisationsansätzen herzustellen.

Der zweite Teil befasst sich mit der Optimierung der Stempel, welche zum molekularen Prägen der Dünnschichten mit Silbernanopartikeln verwendet wurden. Es wurden Glasstempel und PDMS-Stempel verwendet. Beide müssen mit APTES modifiziert werden, um die Nanopartikel zu immobilisieren. Die freien Aminogruppen von APTES reagieren mit den Isocyanaten des Polyurethan-Ansatzes. Die Stempel werden also an die Polymerschicht gebunden und können nicht mehr entfernt werden. Acetaldehyd und Acetanhydrid wurden als Schutzgruppen eingesetzt. Während des Projektes hafteten die Glasstempel auch ohne Schutzgruppe nicht nennenswert am Polymer. Daher konnte nicht festgestellt werden, ob die Modifikation erfolgreich war. Weder auf Polyurethan noch auf Poly(styren-co-divinylbenzen) konnten Abdrücke der Nanopartikel gefunden werden.

Im Gegensatz dazu hafteten unbehandelte PDMS-Stempel auf PU. Nachdem sie mit Acetanhydrid behandelt wurden, konnten die Stempel problemlos vom Polymer entfernt werde. Jedoch lösten sich die Nanopartikel vom Stempel und steckten im Polymer fest. Auch durch längeres Waschen und die Herstellung dünnerer Schichten, konnten die Partikel nicht entfernt werden. Eine Behandlung der Proben mit Salpetersäure, um die Nanopartikel aufzulösen, erzielte bessere Ergebnisse. Jedoch konnten die Partikel nicht restlos entfernt werden.

Die PDMS-Stempel wurden ebenfalls auf Poly(styren-co-divinylbenzen) getestet. Dafür wurden Stempel ohne Schutzgruppe und solche, die mit Acetanhydrid modifiziert wurden, verwendet. Wie bei Polyurethan lösten sich die Nanopartikel von den behandelten PDMS-Stempeln und steckten im Polymer. Die unbehandelten Stempel ließen sich problemlos samt der Nanopartikel entfernen und hinterließen Abdrücke. Waschen war nicht notwendig. Dies leitete zum Schluss, dass die Nanopartikel von Acetanhydrid von den APTES-Molekülen verdrängt werden.

Die oben genannten Ergebnisse verleiten zur Annahme, dass PDMS-Stempel besser für das Molekulare Prägen mit Silbernanopartikeln geeignet sind als Glasstempel. Das könnte auf den Umstand zurückzuführen sein, dass PDMS flexibler ist und besser in Kontakt mit dem Polymer gebracht werden kann. Um die aufgestellten Hypothesen restlos zu verifizieren, sind weitere Experimente auf diesem Gebiet notwendig.